

2018-07

# Separate neural representations of prediction error valence and surprise: Evidence from an fMRI meta-analysis.

Fouragnan, Elsa

<http://hdl.handle.net/10026.1/11506>

---

10.1002/hbm.24047

Human Brain Mapping

Wiley

---

*All content in PEARL is protected by copyright law. Author manuscripts are made available in accordance with publisher policies. Please cite only the published version using the details provided on the item record or document. In the absence of an open licence (e.g. Creative Commons), permissions for further reuse of content should be sought from the publisher or author.*

**HUMAN BRAIN MAPPING****Separate neural representations of prediction error valence  
and surprise: evidence from an fMRI meta-analysis**

Journal:	<i>Human Brain Mapping</i>
Manuscript ID	HBM-17-1205.R2
Wiley - Manuscript type:	Research Article
Date Submitted by the Author:	n/a
Complete List of Authors:	Fouragnan, Elsa; University of Oxford, Experimental Psychology Retzler, Chris; University of Huddersfield, Psychology Philiastides, Marios G; University of Glasgow,
Keywords:	meta-analysis, learning, decision making, reward, prediction error

SCHOLARONE™  
Manuscripts

view

1  
2  
3  
4  
5  
6  
7  
8  
9  
10  
11  
12  
13  
14  
15  
16  
17  
18  
19  
20  
21  
22  
23  
24  
25  
26  
27  
28  
29  
30  
31  
32  
33  
34  
35  
36  
37  
38  
39  
40  
41  
42  
43  
44  
45  
46  
47  
48  
49  
50  
51  
52  
53  
54  
55  
56  
57  
58  
59  
60

1 **Title: Separate neural representations of prediction error valence and surprise:**  
2 **evidence from an fMRI meta-analysis**

4 **Short title:** Separate neural correlates of prediction error valence and surprise

6 **Authors:** Elsa Fouragnan<sup>1,2</sup>, Chris Retzler<sup>1,3</sup> and Marios G. Philiastides<sup>1</sup>

8 **Affiliations:** <sup>1</sup>Institute of Neuroscience & Psychology, University of Glasgow, Glasgow, UK.

9 <sup>2</sup>Department of Experimental Psychology, University of Oxford, Oxford, UK, <sup>3</sup>Department of  
10 Behavioural & Social Sciences, University of Huddersfield, Huddersfield, UK.

12 **Acknowledgements:** Funding for this work was provided by the Biotechnology and  
13 Biological Sciences Research Council (BBSRC; grants BB/J015393/1–2 to M.G.P.) and the  
14 Economic and Social Research Council (ESRC; grant ES/L012995/1 to M.G.P.). We also  
15 thank Dr. Andrea Pisauro, Dr. Miriam Klein-Flugge and Dr. Jacqueline Scholl for helpful  
16 comments on the manuscript.

1  
2  
3 18 **Abstract**  
4  
5 19

6  
7 20 Learning occurs when an outcome differs from expectations, generating a reward prediction  
8  
9 21 error signal (RPE). The RPE signal has been hypothesized to simultaneously embody the  
10  
11 22 valence of an outcome (better or worse than expected) and its surprise (how far from  
12  
13 23 expectations). Nonetheless, growing evidence suggests that separate representations of the  
14  
15 24 two RPE components exist in the human brain. Meta-analyses provide an opportunity to test  
16  
17 25 this hypothesis and directly probe the extent to which the valence and surprise of the error  
18  
19 26 signal are encoded in *separate* or *overlapping* networks. We carried out several meta-  
20  
21 27 analyses on a large set of fMRI studies investigating the neural basis of RPE, locked at  
22  
23 28 decision outcome. We identified two valence learning systems by pooling studies searching  
24  
25 29 for differential neural activity in response to *categorical* positive-vs-negative outcomes. The  
26  
27 30 first valence network (negative > positive) involved areas regulating alertness and switching  
28  
29 31 behaviors such as the midcingulate cortex, the thalamus and the dorsolateral prefrontal  
30  
31 32 cortex whereas the second valence network (positive > negative) encompassed regions of  
32  
33 33 the human reward circuitry such as the ventral striatum and the ventromedial prefrontal  
34  
35 34 cortex. We also found evidence of a largely distinct surprise-encoding network including the  
36  
37 35 anterior cingulate cortex, anterior insula and dorsal striatum. Together with recent animal  
38  
39 36 and electrophysiological evidence this meta-analysis points to a sequential and distributed  
40  
41 37 encoding of different components of the RPE signal, with potentially distinct functional roles.  
42  
43 38  
44  
45  
46  
47  
48  
49  
50  
51  
52  
53  
54  
55  
56  
57  
58  
59  
60

## 39 Introduction

40

41 Effective decision-making depends upon accurate outcome representations associated with  
42 potential choices. These representations can be defined through reinforcement learning (RL)  
43 [Rescorla and Wagner, 1972; Sutton, 1998], a modelling framework that uses the reward  
44 prediction error (RPE), the difference between actual and expected outcomes, as a learning  
45 signal to update future outcome expectations. In this framework, RPE is a signed quantity  
46 and learning is driven by two separate components of the RPE signal: its *valence* (i.e. the  
47 sign of the RPE, representing whether an outcome is better [+] or worse [-] than expected)  
48 and its *surprise* (i.e. the modulus of the RPE, representing the degree [high or low] of  
49 deviation from expectations). Whereas the valence informs an agent whether to reinforce or  
50 extinguish a certain behaviour [Fouragnan et al., 2015; Fouragnan et al., 2017; Frank et al.,  
51 2004], the surprise component determines the extent to which the strength of association  
52 between outcome and expectations needs to be adjusted [Collins and Frank, 2016; Niv et  
53 al., 2015; den Ouden et al., 2012].

54

55 This modelling framework has received considerable attention in neuroscience since the  
56 early 90's when animal neurophysiological studies identified dopaminergic neurons in the  
57 midbrain, in particular in the ventral tegmental area (VTA), the substantia nigra pars  
58 compacta (SNc) and reticulata (SNr), whose tonic response profile appears to  
59 simultaneously capture both components of the RPE signal outlined above [Montague et al.,  
60 1996; Schultz et al., 1993; Schultz et al., 1997]. Specifically, these neurons show  
61 anticipatory increase and suppression of their tonic activity in response to positive and  
62 negative RPE respectively. While the anticipatory increase is proportional to the magnitude  
63 of positive RPE, the magnitude of negative RPE is encoded by the duration of the basal  
64 tonic suppression.

65

1  
2  
3 66 This discovery was a breakthrough in the field of learning and decision making and has  
4  
5 67 continued to be influential in the field over the past two and half decades (see [Schultz,  
6  
7 68 2016a; Schultz, 2016b] for a review). As a result, this neurophysiological work has strongly  
8  
9 69 motivated human functional magnetic resonance imaging (fMRI) research to identify the  
10  
11 70 corresponding macroscopic Blood-Oxygen-Level-Dependent (BOLD) pattern of the signed  
12  
13 71 RPE. This pattern of activity was expected to be such that the strength of the BOLD would  
14  
15 72 proceed from high positive RPEs > low positive RPEs > low negative RPEs > high negative  
16  
17 73 RPEs. More specifically, studies have employed a model-based fMRI approach, whereby  
18  
19 74 different types of reinforcement-learning models are first fitted to subjects' behavior to yield  
20  
21 75 parametric predictors for signed RPE against which fMRI data are subsequently regressed  
22  
23 76 [Daw et al., 2011; Fouragnan et al., 2013; Gläscher et al., 2010; O'Doherty et al., 2004;  
24  
25 77 O'doherty et al., 2007; Queirazza et al., 2017].  
26  
27 78

28  
29 79 These fMRI studies have employed different algorithms to derive the signed RPE, ranging  
30  
31 80 from the simple formulation of the temporal difference learning algorithm to incorporating  
32  
33 81 action learning, notably using the Q-learning and SARSA ('state, action, reward, state, and  
34  
35 82 action') algorithms [Schonberg et al., 2010; Seymour et al., 2007; Tanaka et al., 2006].  
36  
37 83 According to qualitative reviews of this previous findings [O'doherty et al., 2007] as well as  
38  
39 84 quantitative, coordinate-based meta-analyses of these studies, the regions correlating with  
40  
41 85 the different formulations of signed RPE have been found to be predominantly subcortical,  
42  
43 86 including the striatum and amygdala, with some cortical regions, such as the ventromedial  
44  
45 87 prefrontal cortex and the cingulate cortex also reported [Bartra et al., 2013; Garrison et al.,  
46  
47 88 2013; Liu et al., 2011]. Additionally, substantial effort has been undertaken to identify how  
48  
49 89 different types of outcomes (primary reward such as food, or secondary reward such as  
50  
51 90 monetary outcomes) can modulate signed RPE in the same regions and the extent to which  
52  
53 91 it can be considered a domain-general, common currency signal [Sescousse et al., 2013].  
54  
55 92

1  
2  
3 93 While using trial-by-trial estimates of signed RPE from reinforcement-learning models has  
4  
5 94 provided an enormously productive framework for understanding learning and decision-  
6  
7 95 making, a growing number of studies have also discussed the complementary role of  
8  
9 96 surprise, namely the unsigned RPE, which can also be estimated at the single-trial level.  
10  
11 97 These include, but are not limited to, the use of trial-by-trial estimates of the modulus of RPE  
12  
13 98 or Bayesian surprise according to Bayesian learning theory [Hayden et al., 2011; Iglesias et  
14  
15 99 al., 2013]. Additionally, human electroencephalography (EEG) studies, attempting to offer a  
16  
17 100 temporal account of the cortical dynamics associated with RPE processing, did not find a  
18  
19 101 systematic monotonic response profile consistent with a single RPE representation but  
20  
21 102 instead offered evidence suggestive of separate representations for valence and surprise at  
22  
23 103 the macroscopic level of responses recorded on the scalp. Specifically, multiple recent EEG  
24  
25 104 studies combining model-based RPE estimates with single-trial analysis of the EEG revealed  
26  
27 105 an early outcome stage reflecting a purely categorical valence signal and a later processing  
28  
29 106 stage reflecting separate representations for valence and surprise [Fouragnan et al., 2015;  
30  
31 107 Fouragnan et al., 2017; Philiastides et al., 2010b]. These later valence and surprise signals  
32  
33 108 appeared in spatially distinct but temporally overlapping EEG signatures.  
34  
35 109  
36  
37 110 These findings suggest that, in addition to the fully monotonic firing pattern of midbrain  
38  
39 111 neurons, there exist individual representations for valence and surprise, potentially  
40  
41 112 subserving different functional roles during reward-based learning (e.g. approach-avoidance  
42  
43 113 behavior and the speed of learning via varying degrees of attentional engagement,  
44  
45 114 respectively). Here, we conducted an fMRI meta-analysis to explore the possibility that there  
46  
47 115 exist separate neuronal representations encoding valence and surprise promoting reward  
48  
49 116 learning in humans. We discuss the findings of our work in the context of recent reports from  
50  
51 117 animal neurophysiology and human neuroimaging experiments that provide evidence  
52  
53 118 towards a distributed coding of the different facets of the RPE signal [Brischoux et al., 2009;  
54  
55 119 Fouragnan et al., 2015; Fouragnan et al., 2017; Matsumoto and Hikosaka, 2009].  
56  
57  
58  
59  
60

1  
2  
3 1204  
5 121 **Materials and Methods**6  
7 122

8  
9 123 **Literature search.** We selected fMRI studies using the Pubmed database  
10  
11 124 (<http://www.ncbi.nlm.nih.gov/pubmed>) with the following search keywords: "(fMRI OR  
12  
13 125 neuroimaging) AND (prediction error OR reward OR surprise)" along with three initial filters  
14  
15 126 preselecting studies in which participants were human adults of over 19 years of age and  
16  
17 127 excluding reviews. This initial selection resulted in 724 candidates for inclusion to which a  
18  
19 128 further twenty papers were added from existing in-house reference libraries. Note that  
20  
21 129 previous meta-analyses used the terms "prediction error" or "reward" but we are the first to  
22  
23 130 include "surprise" in our systematic search for relevant papers [Bartra et al., 2013; Garrison  
24  
25 131 et al., 2013; Sescousse et al., 2013].

26  
27 132

28  
29 133 Abstracts from the 788 candidate-papers identified were then evaluated for inclusion in the  
30  
31 134 corpus according to the following criteria. We required studies of healthy human adults,  
32  
33 135 reporting changes in BOLD as a function of three different components of RPE: the  
34  
35 136 categorical valence, surprise and signed RPE, including statistical comparisons either in the  
36  
37 137 form of binary contrasts or continuous parametric analyses. Because the main objective of  
38  
39 138 the present meta-analysis is to examine the neural coding of RPE processing at decision  
40  
41 139 outcome, we also imposed the restriction that fMRI analyses were time-locked to the  
42  
43 140 presentation of outcomes (feedback). We used studies involving outcomes consisting of  
44  
45 141 abstract points, monetary payoffs, consumable liquids and arousing pictures but excluded  
46  
47 142 papers in which outcomes consisted of social feedback. We also required that studies used  
48  
49 143 functional brain imaging and did not use pharmacological interventions and ensured that the  
50  
51 144 reported coordinates were either in Montreal Neurological Institute (MNI) or Talairach space.  
52  
53 145 Finally, we excluded papers in which results were derived from region of interest (ROI) since  
54  
55 146 our meta-analytic statistical methods assume that foci are randomly distributed in the whole  
56  
57 147 brain under the null hypothesis. After applying these constraints our meta-analysis



1  
2  
3 148 comprised 102 publications with a total of 2316 participants, 144 contrasts, and 991  
4  
5 149 activation foci. The number of participants per study ranged from 8 to 66 (median = 24,  
6  
7 150 interquartile range [IQR] = 7).  
8  
9 151

10 152 **Study categorization.** The goal of this meta-analysis was to separately categorize studies  
11  
12 153 along the three components of RPE, locked at time of outcome, in order to: 1) identify the  
13  
14 154 extent to which there exist distinct neural representations for valence and surprise and 2)  
15  
16 155 identify whether the neural correlates of the signed RPE simply intersect those of valence  
17  
18 156 and surprise (possibly due to colinearities across these components) or appear as unique  
19  
20 157 clusters of activation reflecting the true combined influence of the two measures.  
21  
22 158

23  
24 159 To group the relevant papers according to the three main RPE components we used the  
25  
26 160 following definitions: 1) *valence* represents the sign of the RPE and as such it is positive  
27  
28 161 when an outcome is better than expected and negative when worse than expected, 2)  
29  
30 162 *surprise* represents the absolute degree of deviation from expectations and is treated as an  
31  
32 163 unsigned quantity and 3) *signed RPE* simultaneously reflects the influence of both valence  
33  
34 164 and surprise and appears as a fully signed parametric signal. According to these definitions,  
35  
36 165 we identified several fMRI statistical analyses conducted in the original studies that fall under  
37  
38 166 each of the three RPE components (Table 1). The main assumptions of these fMRI  
39  
40 167 analyses, with regard to the BOLD signal as a function of each RPE component, are  
41  
42 168 presented schematically in Figure 1.  
43  
44 169

45  
46 170 [Figure 1]  
47  
48 171

49  
50 172 For the valence components, the literature has looked at neural responses which vary  
51  
52 173 categorically along positive-negative axes, as represented in patterns A (i) and (ii) of Figure  
53  
54 174 1. We therefore extracted activations exhibiting a relative BOLD signal increase for negative  
55  
56 175 relative to positive outcomes (NEG > POS: pattern A (i)) and greater BOLD for positive  
57  
58  
59  
60

1  
2  
3 176 relative to negative outcomes (POS > NEG: pattern A (ii)), respectively. We considered six  
4  
5 177 types of fMRI statistical comparisons which reported coordinate results from either: (1) a  
6  
7 178 contrast associated with negative > positive outcomes, (2) a contrast associated with  
8  
9 179 negative > no outcomes, (3) a negative correlation with a trial-by-trial regressor modulated  
10  
11 180 by [+1] for positive outcomes and [-1] for negative outcomes, (4) the positive correlation with  
12  
13 181 the regressor described in (3), (5) a contrast associated with positive > negative outcomes  
14  
15 182 and (6) a contrast associated with positive > no outcomes. We grouped results from  
16  
17 183 contrasts 1-3 (i.e. NEG > POS) and contrasts 3-6 (i.e. POS > NEG) to capture regions  
18  
19 184 yielding greater BOLD activity for negative relative to positive outcomes and a greater  
20  
21 185 activity for positive relative to negative outcomes respectively (Table 1).  
22  
23 186

24  
25 187 While the fMRI literature on RPE processing has produced a large amount of theoretical and  
26  
27 188 empirical evidence for the valence and the signed RPE components, comparatively little has  
28  
29 189 been done to directly investigate surprise as a separate component. Fewer studies have  
30  
31 190 used fMRI regressors that were parametrically modulated by trial-to-trial changes in surprise  
32  
33 191 using the unsigned RPE [Fouragnan et al., 2017; Hayden et al., 2011; Iglesias et al., 2013].  
34  
35 192 These studies used the terms "surprise", "unsigned RPE", or outcome "saliency" to refer to  
36  
37 193 the mathematical modulus of RPE from computational learning models. In addition to these  
38  
39 194 papers, our literature search has revealed a number of other measures (see below), which  
40  
41 195 are highly correlated with outcome surprise, as defined by learning theory. We therefore  
42  
43 196 used these measures as proxies of surprise to gain insights into the spatial extent of the  
44  
45 197 relevant neural responses and the degree to which they overlap with those associated with  
46  
47 198 valence.  
48  
49 199

50  
51 200 Specifically, a recent line of research has investigated the neural basis of "Bayesian  
52  
53 201 surprise" or "volatility", computed as the direct modulus of Bayesian predictive error [Ide et  
54  
55 202 al., 2013; Iglesias et al., 2013; Mathys et al., 2014; O'Reilly et al., 2013] which correspond to  
56  
57 203 the absolute difference between categorical outcomes and the probabilistic expectation of  
58  
59  
60

1  
2  
3 204 these outcomes, estimated using Bayesian inference. In the framework of Bayesian learning,  
4  
5 205 the absolute Bayesian RPE plays an important role in learning from rapid changes in  
6  
7 206 behavioral exploration [Courville et al., 2006]. Finally, other studies used the term  
8  
9 207 “associability” which is a parameter in the Pearce-Hall model [Hall and Pearce, 1979; Pearce  
10  
11 208 and Hall, 1980] defined as the degree of divergence between an actual outcome and the  
12  
13 209 original expectation (e.g., the associative strength between a choice and an outcome). We  
14  
15 210 note however, that in the RL framework, associability can also refer to the learning rate. It is  
16  
17 211 clear from these reports that there is a lack of consistent terminology to refer to unsigned  
18  
19 212 RPE, which emphasizes the need for a more unified framework for studying RPE  
20  
21 213 processing.

22  
23 214  
24  
25 215 To test for consistencies in the neuronal responses across these different reports, and  
26  
27 216 provide initial support for a unified representation of surprise, we grouped fMRI analyses  
28  
29 217 which reported outcome-locked activations resulting from: (1) a positive correlation with a  
30  
31 218 trial-by-trial regressor of the modulus (unsigned) RPE resulting from RL models across both  
32  
33 219 positive and negative outcomes (“surprise” or “unsigned RPE”), (2) a positive correlation  
34  
35 220 with a trial-by-trial regressor of the unsigned RPE resulting from Bayesian modelling  
36  
37 221 (“Bayesian Surprise” or “volatility”), (3) a positive correlation with a trial-by-trial regressor of  
38  
39 222 the free parameter of the Pearce-Hall model (“associability” term), (4) a contrast associated  
40  
41 223 with (high positive outcomes and high negative outcomes) > (low positive outcomes and low  
42  
43 224 negative outcomes OR no outcomes), (5) a positive correlation with a parametric regressor of  
44  
45 225 surprising positive RPE alone and (6) a positive correlation with a parametric regressor of  
46  
47 226 surprising negative RPE alone (Table 1). Figure 1 illustrates the hypothesized pattern of  
48  
49 227 BOLD signal predicted by these contrasts (pattern B), exhibiting a V shaped response profile  
50  
51 228 that is maximal for both highly surprising negative and positive RPEs. Despite possible  
52  
53 229 subtle differences in the definition of these measures we expected that only foci consistently  
54  
55 230 correlating with deviations from reward expectations would be revealed in this analysis.

56  
57 231

1  
2  
3 232 One reason the surprise component has not been looked at closely in isolation is because  
4  
5 233 the literature has focused primarily on signed RPE representations instead. This approach  
6  
7 234 was motivated by neurophysiology experiments showing monotonic responses as a function  
8  
9 235 of both valence and surprise and by a theoretical framework suggesting that learning is  
10  
11 236 driven by a single signed RPE representation. To identify the spatial extent of these  
12  
13 237 representations we also looked at fMRI data reporting positive correlations with signed RPE  
14  
15 238 (negative correlation were discarded). Specifically, we combined four types of fMRI  
16  
17 239 analyses, which estimated trial-by-trial signed RPE from different computational models. We  
18  
19 240 used fMRI reports from (1) model-free and (2) model-based RL methods. Model-free  
20  
21 241 methods include Markov Chain Monte Carlo and temporal difference methods [Samson et  
22  
23 242 al., 2010; Seymour et al., 2007]. Model-based methods include dynamic programming and  
24  
25 243 certainty equivalent methods [Daw et al., 2005; Doya et al., 2002]. More on these algorithms  
26  
27 244 can be found in the review by [Kaelbling et al., 1996]. We also included continuous  
28  
29 245 parametric analyses using trial-by-trial signed RPE from (3) Bayesian RL framework  
30  
31 246 described above [Iglesias et al., 2013; Mathys et al., 2014; den Ouden et al., 2012]. Finally,  
32  
33 247 our analysis for signed RPE also contained one type of parametric analysis that employed  
34  
35 248 fixed RPE values (not estimated from RL models) ranked on a scale such that (4) high  
36  
37 249 positive RPEs > low positive RPEs > low negative RPEs > high negative RPEs (Table 1).  
38  
39 250 Figure 1 illustrates the hypothesized pattern of BOLD signal predicted by these contrasts  
40  
41 251 (pattern C) and it is assumed to increase linearly as a function of signed RPE.

42  
43 252

44  
45 253 Crucially, we note that an issue requiring closer scrutiny pertains to the difficulty in  
46  
47 254 disambiguating the signed RPE pattern of activity from those associated with valence and  
48  
49 255 surprise. Specifically, pattern C (signed RPE) is generally highly correlated with pattern A (ii),  
50  
51 256 (POS > NEG valence) and in studies in which only positive RPEs are considered, pattern C  
52  
53 257 (signed RPE) and pattern B (surprise) are perfectly correlated. Nonetheless, comparing  
54  
55 258 clusters of activations across the three RPE components could potentially reveal whether or  
56  
57 259 not there exist unique clusters of activations associated with signed RPE.

1  
2  
3 2604  
5 261 [Table 1]6  
7 2628  
9 263 **2.1. Activation Likelihood Estimation (ALE) analysis**10  
11 264

12 265 We conducted the meta-analysis using the GingerALE software (version 2.3.6) [Eickhoff et  
13 al., 2009] that employs a revised (and rectified [Eickhoff et al., 2017]) version of the  
14 266 activation likelihood estimation (ALE) algorithm [Laird et al., 2005; Turkeltaub et al., 2002],  
15 267 which identifies common areas of activation across studies. This method performs  
16 268 coordinate based meta-analysis which considers each reported foci as a 3D Gaussian  
17 269 probability distribution, centred at the coordinates provided by each study reflecting the  
18 270 spatial uncertainty associated with each reported set of coordinates. Note that each contrast  
19 271 provided to the ALE algorithm is treated as a separate experiment. The probabilities  
20 272 distributions are then combined to create a modelled activation map, namely an ALE map for  
21 273 that contrast. Studies are weighted according to the number of subjects they contain by  
22 274 adjusting the full width at half maximum of the Gaussian distributions. The convergence of  
23 275 results across the whole brain is obtained by computing the union of all resulting voxel-wise  
24 276 ALE scores. To distinguish meaningful convergence from random noise, statistics are  
25 277 computed by comparing ALE scores with an empirical null-distribution representing a  
26 278 random spatial association between studies. To infer true convergence, a random-effect  
27 279 inference is applied to capitalize on the differences between studies rather than between foci  
28 280 within a particular study. The null-hypothesis is modelled by randomly sampling voxels from  
29 281 each of the ALE maps from which the union is obtained. The ALE maps are assessed  
30 282 against the null distribution using a cluster level threshold of specific p-values. Contrast  
31 283 analyses between categories of the entire dataset are determined by ALE subtraction  
32 284 method, including a correction for differences in sample size between the categories.  
33 285  
34 286

35  
36  
37  
38  
39  
40  
41  
42  
43  
44  
45  
46  
47  
48  
49  
50  
51  
52  
53  
54  
55  
56  
57  
58  
59  
60

1  
2  
3 287 Here, we manually extracted all coordinates from the studies shown in Table 1 and entered  
4  
5 288 them into separate files for each of the three RPE components in preparation for the ALE  
6  
7 289 analyses. Any studies that provided coordinates in Talairach space were converted into MNI  
8  
9 290 space by the Matlab (MathWorks, Natick, Massachusetts) function *tal2mni* in the fieldtrip  
10  
11 291 toolbox [Oostenveld et al., 2011]. We conducted ALE analyses for each of the three  
12  
13 292 components of RPE individually. Along the valence component, we looked at both patterns A  
14  
15 293 (i) and A (ii) in Figure 1 (i.e. to identify activations for negative > positive RPE and vice  
16  
17 294 versa, respectively). Accordingly, we ran separate ALE analyses for each of the two  
18  
19 295 patterns. In addition, we performed two conjunction analyses – one between the valence and  
20  
21 296 surprise components to investigate our hypothesis of largely separate neural representations  
22  
23 297 and another between all three RPE components to identify regions that simultaneously  
24  
25 298 encode these representations. Subsequently, we also performed all possible pairwise  
26  
27 299 contrast analyses between the three patterns (A, B and C), using the individual maps  
28  
29 300 associated with each pattern.

31  
32 301 A total of 402 foci from 66 contrasts were used with 262 foci from 31 contrasts for Pattern A  
33  
34 302 (i) revealing BOLD patterns greater for negative than positive outcomes and 205 from 35  
35  
36 303 contrasts for Pattern A (ii) (e.g. the opposite contrast). For the surprise (Pattern B) and  
37  
38 304 signed RPE (Pattern C) analyses, we applied individual ALE analyses, with 284 foci from 40  
39  
40 305 contrasts for surprise and 240 foci from 38 contrasts for signed RPE. Overall, the number of  
41  
42 306 contrasts used for each separate outcome component was large enough (> 30) to allow  
43  
44 307 sufficient power for the required statistical tests [Eickhoff and Etkin, 2016]. Finally, we  
45  
46 308 transformed the resulting ALE maps from the Colins MNI individual brain space  
47  
48 309 (Colin27\_T1\_seg\_MNI) to the MNI normalized brain space (MNI ICBM152 template) by  
49  
50 310 applying an affine transformation using the FSL *flirt* program [Jenkinson et al., 2002], prior to  
51  
52 311 overlaying onto the canonical MNI template for visualization.

53  
54 312

### 55 313 **3. Results**

56  
57  
58  
59  
60

314

315 All coordinates used for the following ALE analyses were collated from fMRI studies in which  
316 the components of RPE have been regressed onto BOLD activity time-locked to outcome  
317 presentation. We report ALE maps with clusters surviving the False Discovery Rate (FDR)  
318 yielding two p-value thresholds. The most conservative FDR correction yields a p-value with  
319 no assumptions about how the data is correlated (FRN), and the least conservative FDR  
320 correction assumes independence or positive dependence (FID) with  $p < 0.05$  and a  
321 minimum volume clustering value of  $50 \text{ mm}^3$ . Note that, using a cluster-level family-wise  
322 error (FWE) correction implemented with a cluster-extent threshold of  $p < 0.05$  and a cluster-  
323 forming threshold of  $p < 0.001$  revealed virtually identical results (compared with FRN)  
324 [Eickhoff et al., 2017] as per previous reports [R Garrison et al., 2017]. For all tables  
325 presenting ALE cluster results, the size of each cluster is provided in  $\text{mm}^3$  along with the  
326 associated MNI coordinates and maximum ALE score. The ALE score indicates the relative  
327 effect size for each peak voxel within each ALE analysis.

328

### 329 3.1. Outcome Valence

330

331 The first two ALE analyses were conducted to identify regions in which BOLD signals  
332 correlate with outcome valence. Specifically, we looked at activations that yielded greater  
333 BOLD for negative relative to positive outcomes (NEG > POS; pattern A (i) in Figure 1) and  
334 greater BOLD for positive relative to negative outcomes (POS > NEG; pattern A (ii) in Figure  
335 1), respectively. Accordingly, we considered all fMRI studies, which assumed BOLD  
336 responses varying categorically along a positive-negative axis for outcome valence.

337

338 The findings of the two valence ALE analyses are shown in Figure 2. The resulting maps  
339 revealed a highly distributed network of brain activations encompassing several cortical  
340 regions and sub-cortical structures. More precisely, NEG > POS valence clusters were found

1  
2  
3 341 in a network encompassing the anterior and dorsal part of the mid-cingulate cortex (aMCC  
4 342 and dMCC) including the pre supplementary motor area (pre-SMA), the bilateral anterior and  
5 343 middle insular cortex (aINS, mINS), the bilateral dorsolateral prefrontal cortex (dlPFC), the  
6 344 bilateral thalamus, right amygdala, left inferior parietal lobule (IPL) and the habenula.  
7  
8  
9

10  
11 345  
12 346 POS > NEG valence clusters were found in the bilateral ventral striatum (vSTR), the  
13 347 ventromedial prefrontal cortex (vmPFC), the posterior part of the cingulate cortex (PCC), as  
14 348 well as the ventrolateral orbitofrontal cortex (vlOFC). At a lower threshold (uncorrected p-  
15 349 value of 0.001), we also found the midbrain as part of this network, encompassing the VTA,  
16 350 which is commonly associated with the delivery of reward [D'Ardenne et al., 2008]. Table 2  
17 351 contains the complete list of regions, coordinates, and statistics of these two ALE analyses.  
18  
19  
20  
21  
22  
23  
24  
25

26 352  
27 353 [Figure 2], [Table 2]  
28  
29

### 30 354 31 355 **3.2. Surprise** 32 33

34 356  
35 357 FMRI investigations of RPE have focused primarily on the valence components while  
36 358 neglecting potential contributions from possible separate representations along the surprise  
37 359 component, defined as the degree by which outcomes deviate from expectations and  
38 360 mathematically expressed as the modulus of RPE. A major goal of this work was to explore  
39 361 the possibility that there exist largely separate neuronal representations encoding surprise.  
40 362 To this end, we conducted a new ALE analysis in which the few empirical fMRI studies  
41 363 making use of the surprise from RL models were combined with other fMRI measures  
42 364 correlated with the surprise as defined by RL models (Table 1).  
43  
44  
45  
46  
47  
48  
49

50 365  
51 366 Figure 3 shows the areas in which BOLD signal correlated with surprise. We found evidence  
52 367 for activations in a distributed network encompassing the aMCC, dMCC, the pre-SMA the  
53 368 bilateral dorsal striatum (dSTR), the bilateral aINS, the MTG and the midbrain. Crucially, this  
54  
55  
56  
57  
58  
59  
60



1  
2  
3 369 activation map shows that the neural network associated with surprise is largely distinct from  
4  
5 370 that of valence. This finding provides initial support for the notion that these two RPE  
6  
7 371 components are encoded in separate brain areas and, as such, they might be contributing  
8  
9 372 individually to promote learning. The full results of the surprise ALE analysis are also  
10  
11 373 summarized in Table 3.

12  
13 374

14  
15 375 [Figure 3], [Table 3]

16  
17 376

### 18 377 **3.3. Valence and surprise conjunction and contrast analyses**

19  
20  
21 378

22  
23 379 The activation maps for valence (NEG > POS and POS > NEG) and surprise ALE analyses  
24  
25 380 conducted above revealed little overlap between the spatial representations of these two  
26  
27 381 RPE components. To formally quantify the degree of overlap between the valence and  
28  
29 382 surprise networks, we next ran a conjunction analysis between the two components. The  
30  
31 383 statistical map resulting from this conjunction analysis and the two separate statistical maps  
32  
33 384 of valence and surprise (as already reported in Figures 2 and 3) are overlaid in Figure 4.

34  
35 385

36  
37 386 [Figure 4], [Table 4]

38  
39 387

40  
41 388 Contrast analyses were conducted for each possible pairing between any dimensions of  
42  
43 389 valence (POS > NEG [positive]; NEG > POS [negative] and POS + NEG [all valence]) and  
44  
45 390 surprise. These analyses allowed us to identify the areas that were unique and specific to  
46  
47 391 each individual outcome and RPE-related component. The positive valence (pattern A (ii))  
48  
49 392 minus surprise (pattern B) contrast revealed two main clusters in the vSTR and vmPFC  
50  
51 393 whereas the reverse contrast revealed a network of clusters including preSMA, aINS, and  
52  
53 394 MTG. Contrasting negative valence (pattern A (i)) and surprise also exposed separate  
54  
55 395 networks of areas for each subtraction. Specifically, this contrast revealed a network  
56  
57 396 encompassing the thalamus, the habenula, the right mINS and the dmCC, whereas the

1  
2  
3 397 reverse contrast showed clusters in the dorsal portion of the STR and the dlPFC. The  
4  
5 398 statistical maps resulting from these contrast analyses are presented in Figure 5.

6  
7 399

8  
9 400 [Figure 5], [Table 5]

10  
11 401

### 12 402 **3.4. Signed RPE**

13  
14  
15 403

16  
17 404 A major goal of this work was to investigate the spatial profile of the signed RPE component  
18  
19 405 and to scrutinise more closely the extent to which it overlaps with the separate  
20  
21 406 representations identified for valence (NEG > POS and POS > NEG) and surprise. The  
22  
23 407 fMRI-RPE literature has focused on this component largely due to neurophysiological  
24  
25 408 evidence suggesting that RPE-like learning is driven by a single, theoretically unified  
26  
27 409 representation of both POS > NEG valence and surprise (Table 1).

28  
29 410

30  
31 411 Results from this ALE analysis revealed very few unique activations for signed RPE  
32  
33 412 compared to valence and surprise. Instead, brain areas identified in this analysis overlapped  
34  
35 413 mostly with areas appearing in the POS > NEG valence component and, to a lesser extent,  
36  
37 414 surprise (Figure 6). Specifically, a large overlap between signed RPE and the POS > NEG  
38  
39 415 valence component was found in the STR and a smaller one in the vmPFC. Similarly, areas  
40  
41 416 appearing in the signed RPE analysis that overlapped with the surprise component were  
42  
43 417 also found, albeit only in small clusters comprising the aMCC and dorsal STR. Taken  
44  
45 418 together, these findings emphasize the potential collinearities between the BOLD predictors  
46  
47 419 used to identify neural representations associated with the three RPE components and  
48  
49 420 highlight the need for developing a methodology for properly disentangling their individual  
50  
51 421 contributions.

52  
53 422

54  
55 423 [Figure 6], [Table 6]

56  
57 424

### 425 **3.5. Putting it all together**

426

427 Subsequently, to formally test for the overlap between all three RPE components and  
428 identify potential regions integrating valence and surprise either into a signed RPE  
429 representation or a linear superposition of the two signals [Fouragnan et al., 2017], we  
430 performed a conjunction analysis between the valence (pattern A), the surprise (pattern B)  
431 and signed RPE (pattern C) signals. We summarize our conjunction results in Figure 7,  
432 which revealed a major overlap between all activations associated with signed RPE and  
433 each of the other two RPE representations in the central part of the STR. Thus, one  
434 possibility is that the STR meets the requirement that a full monotonic representation of the  
435 error signal also simultaneously encodes valence and surprise, as per our last ALE analysis.

436

437 [Figure 7]

438

439 Another possibility is that the overlap between all components of outcomes in the STR is  
440 arising, at least in part, due to collinearities across the different outcome representations,  
441 particularly between the positive categorical nature of outcome valence (pattern A (ii)) and  
442 the signed RPE. To formally test this hypothesis, we performed a new series of contrast  
443 analyses between signed RPE and all dimensions of categorical valence and surprise.  
444 Particularly, we performed contrast analyses between patterns C-A(i), C-A(ii), C-A and C-B  
445 (and vice versa). The results are summarized in Figure 8. Particularly, we did not find any  
446 area unique to signed RPE when looking at each of the individual comparisons of signed  
447 RPE with the other three patterns. In fact, when comparing signed RPE to positive valence  
448 (pattern A (ii)), no clusters were found to be significantly different than those found with the  
449 categorical outcome valence (POS > NEG). Conversely, the STR was found for all the other  
450 signed RPE comparisons (signed RPE > negative; signed RPE > surprise). Finally, the  
451 unique network related to negative valence (pattern A (i)) was found in the dMCC, thalamus

1  
2  
3 452 and mINS, the unique cluster related to positive valence was found in the vmPFC and the  
4  
5 453 unique network related to surprise was found in the aMCC, preSMA and the aINS.

6  
7 454

8  
9 455 [Figure 8], [table 7]

10  
11 456

## 12 457 **Discussion**

13  
14  
15 458

16  
17 459 In this fMRI meta-analysis work, we demonstrated that reward learning in humans involves  
18  
19 460 separate neuronal signatures of RPE, comprising distinct representations for valence and  
20  
21 461 surprise. Together with recent neurophysiological and EEG evidence (including studies  
22  
23 462 using simultaneous EEG and fMRI), these findings point to a potentially sequential and  
24  
25 463 distributed encoding of different RPE components with potentially functionally distinct roles.

26  
27 464

### 28 465 **Valence networks**

29  
30  
31 466

32  
33 467 The ALE analyses related to valence revealed two distributed set of activations correlating  
34  
35 468 with both pattern A (i) and (ii) in Figure 1. Foci for which the BOLD signal was greater for  
36  
37 469 negative than positive outcomes showed significant clustering in a large network of areas  
38  
39 470 including the thalamus, the aMCC and dMCC, the aINS, mINS and the dIPFC. Conversely,  
40  
41 471 foci for which the BOLD signal was greater for positive than negative outcomes showed  
42  
43 472 significant clusters in a separate network including vmPFC, vSTR, PCC, and vIOFC. These  
44  
45 473 findings clearly suggest the presence of multiple systems responding to the categorical  
46  
47 474 nature of valence which supports the notion that separate valuation systems shape learning  
48  
49 475 in the human brain [Fiorillo, 2013; Fouragnan et al., 2013], although their functional role  
50  
51 476 remain debated. More specifically, the debate focuses on the number and exact nature of  
52  
53 477 the neural systems assigning value to decision outcomes and driving behaviors that are  
54  
55 478 evolutionarily appropriate in response to changes in the environment.

56  
57 479  
58  
59  
60

1  
2  
3 480 A first theory describes two distinct valence systems invoking two orthogonal axes of  
4  
5 481 decision-making: alertness (involving the implementation of action) and learning (including  
6  
7 482 the updates of value expectations for future avoidance and approach behaviors). In this  
8  
9 483 framework, the first system is thought to monitor on-going activity and interrupt it when  
10  
11 484 needed to trigger switching behaviors (e.g. following negative RPEs). In contrast, the second  
12  
13 485 system uses both negative and positive RPE values for decreasing or increasing internal  
14  
15 486 value representations associated with decisions to ultimately drive avoidance and approach  
16  
17 487 learning, respectively [Boureau and Dayan, 2011; Cools et al., 2011; Elliot, 2006; Fiorillo,  
18  
19 488 2013; Fouragnan et al., 2015; Gray and McNaughton, 2003; Guitart-Masip et al., 2012].

20  
21 489  
22  
23 490 A second (not mutually exclusive) proposition supports the idea that there are at least two  
24  
25 491 separate systems responsible for aversive and appetitive reinforcements such that  
26  
27 492 punishments and rewards are encoded separately (i.e. a punishment space and a reward  
28  
29 493 space [Morrens, 2014]). This proposition was developed on the basis of neurophysiological  
30  
31 494 evidence showing that different types of neurons exhibit differential activity in response to  
32  
33 495 punishing vs. non-punishing outcomes and rewarding vs. non-rewarding outcomes,  
34  
35 496 respectively [Fiorillo et al., 2003; Fiorillo, 2013; Schultz et al., 1992; Schultz, 1998]. In this  
36  
37 497 second theory, the punishment space is responsible for avoidance behaviors as well as  
38  
39 498 avoidance learning and the reward space is responsible for approach behaviors and  
40  
41 499 approach learning.

42  
43 500  
44  
45 501 It is noteworthy that our meta-analysis on itself cannot directly distinguish between the two  
46  
47 502 theories because the results do not reveal whether the relevant activations respond  
48  
49 503 exclusively to either positive or negative outcomes or are modulated by both outcomes in  
50  
51 504 opposite directions. This distinction is critical because the former response profile would  
52  
53 505 suggest the presence of separate approach and avoidance systems that might not  
54  
55 506 necessarily be linked to the learning processes as such, while the latter might point to both  
56  
57 507 up- and down-regulation of activity consistent with learning and updating of reward

1  
2  
3 508 expectations. Nonetheless, the meta-analysis results suggest that two main networks  
4  
5 509 process valence. The network encompassing aINS, aMCC, thalamus and dlPFC could  
6  
7 510 regulate on-going activity and alertness or could represent the punishment space in  
8  
9 511 accordance to the first and the second theories respectively. Conversely, the network of  
10  
11 512 regions encompassing the vmPFC, vSTR, PCC and vlOFC could represent the learning  
12  
13 513 system depicted in the first theory or could represent the reward space depicted in the  
14  
15 514 second theory. Further research is required to tease apart the roles of these systems,  
16  
17 515 especially by investigating their precise response profiles in the appetitive (where rewarding  
18  
19 516 and non-rewarding outcomes are manipulated) and in a true aversive (where punishing and  
20  
21 517 non-punishing outcomes are manipulated) domains, respectively.  
22  
23 518

### 24 519 **Surprise network**

25  
26 520  
27  
28 521 Emerging evidence indicates that the brain encodes the unsigned RPE signal (surprise),  
29  
30 522 which alerts the organism of relative deviations from expectations, regardless of the outcome  
31  
32 523 value. However, to date, only few papers have modelled surprise as such to search for  
33  
34 524 independent neural representations, with the exception of recent neurophysiological  
35  
36 525 developments [Brischoux et al., 2009; Matsumoto and Hikosaka, 2009], recent EEG work  
37  
38 526 [Philiastides et al., 2010b; Yeung and Sanfey, 2004] and an increasing number of fMRI  
39  
40 527 studies [Fouragnan et al., 2017; Gläscher et al., 2010; Li and Daw, 2011; Metereau and  
41  
42 528 Dreher, 2013]. Nevertheless, other fMRI studies used variables highly correlated with  
43  
44 529 surprise that can be employed as proxies [Behrens et al., 2007; Iglesias et al., 2013; Nassar  
45  
46 530 et al., 2012; den Ouden et al., 2012; Yu and Dayan, 2005]. These studies share the  
47  
48 531 assumption that the corresponding BOLD response profile is maximal for high positive and  
49  
50 532 high negative RPE and minimal for no RPE, resembling a V-shape, as illustrated with  
51  
52 533 Pattern B in Figure 1. By combining these fMRI results into a single ALE-analysis, we  
53  
54 534 expose for the first time the network associated with surprise while stressing the need for a  
55  
56 535 common lexicon for this learning component to guide subsequent research in the field.  
57  
58  
59  
60

1  
2  
3 536

4 537 The surprise ALE-analysis revealed a large network including cortical and sub-cortical areas  
5  
6 538 such as aMCC, bilateral aINS, dSTR and midbrain, that differed majoritarily from those of  
7  
8 539 valence processing although small overlaps were found between the two components at the  
9  
10 540 junction of ventral and dorsal STR, in left aINS and aMCC. Importantly, the role of surprise is  
11  
12 541 still a subject of debate. Some studies propose that this network encodes the saliency of an  
13  
14 542 outcome or how much a stimulus stands out from others [Litt et al., 2011; Zink et al., 2004].  
15  
16 543 As such, the surprise system could be considered as a key attentional mechanism that  
17  
18 544 enables an organism to focus its limited perceptual and cognitive resources on the most  
19  
20 545 pertinent subset of the available sensory data, similarly to the attentional mechanism used to  
21  
22 546 guide decisions in the case of salient stimuli [Kahnt and Tobler, 2013]. Consistent with a role  
23  
24 547 in attention regulation, representations of such signal have been found in lower-level visual  
25  
26 548 areas [Serences, 2008], lateral intraparietal cortex [Huettel et al., 2006; Kahnt and Tobler,  
27  
28 549 2013] and areas involved in visual and motor preparation such as the supplementary motor  
29  
30 550 area [Wunderlich et al., 2009] or the supplementary eye field [Middlebrooks and Sommer,  
31  
32 551 2012; So and Stuphorn, 2012].  
33

34 552

35  
36 553 In contrast, it has also been suggested that a surprise system can independently monitor  
37  
38 554 unexpected information and act as a learning signal that allows better predictions of  
39  
40 555 upcoming events, and help plan appropriate behavioral adjustments [Dayan and Balleine,  
41  
42 556 2002; Fouragnan et al., 2017; Kolling et al., 2012; Wittmann et al., 2016]. In particular, some  
43  
44 557 studies suggest that the aINS receives information related to surprise and direct modulation  
45  
46 558 from the dSTR providing crucial information for behavioral adjustment [Menon and Levitin,  
47  
48 559 2005]. Along these lines, the surprise signal also captures the essence of a learning signal  
49  
50 560 that the brain needs to compute to maintain a homeostatic state [Friston et al., 2006; Friston,  
51  
52 561 2009]. Practically, this means that the brain elaborates internal predictions about sensory  
53  
54 562 input and updates them according to surprise, a process that can be formulated as  
55  
56 563 generalized Bayesian filtering or predictive coding in the brain. Finally, still in the framework  
57  
58  
59  
60

1  
2  
3 564 of learning, some authors argue that surprise can also be considered as a signal predicting  
4  
5 565 the level of risk associated with a future decision outcome, and thus reflect a risk RPE  
6  
7 566 [Fiorillo et al., 2003; Preuschoff et al., 2008; Rudorf et al., 2012].  
8  
9 567

### 10 568 **Neuromodulatory pathways encoding multicomponent RPE signals**

11  
12 569  
13  
14 570 Supporting the idea of separate neural systems for valence and surprise, recent  
15  
16 571 electrophysiological work has revealed both signals existing in neighbouring groups of  
17  
18 572 neurons. The first study of this kind observed the response of dopaminergic neurons in  
19  
20 573 ventral and dorsal areas of the SNc and reported two categories of dopamine neurons  
21  
22 574 [Matsumoto and Hikosaka, 2009]. Some dopamine neurons increase their phasic firing  
23  
24 575 activity in response to valence while others responded only to the changes in unsigned RPE,  
25  
26 576 regardless of the valence component. The latter population of neurons was located more  
27  
28 577 dorsolaterally in the SNc, whilst the neurons encoding valence were located more  
29  
30 578 ventromedially, including the VTA. Interestingly, the dorsolateral SNc projects mainly to the  
31  
32 579 dorsal STR, whereas the ventral SNc and VTA project to the ventral STR, which matches  
33  
34 580 the results of our last conjunction analysis (Figure 7). We found that the only region that  
35  
36 581 encodes the full monotonic representation of the RPE as well as the separate valence and  
37  
38 582 surprise components of RPE seems to be the central part of the STR as shown in Figure 7.  
39  
40 583 This result aligns with the assumption that this region receives direct projections from the  
41  
42 584 midbrain dopaminergic neurons encoding a fully monotonic signed RPE signal [Schultz et  
43  
44 585 al., 1997]. Additionally, the meta-analysis also revealed that both the valence (POS > NEG)  
45  
46 586 and surprise networks include activity in the midbrain, confirming this hypothesis.  
47  
48 587

49  
50 588 It is important to note that identifying neural activity associated with valence and surprise  
51  
52 589 signals is challenging because in many experimental paradigms both components are highly  
53  
54 590 correlated. For example, when positive RPE are manipulated in isolation, valence (POS >  
55  
56 591 NEG) strongly correlates with surprise. Additionally, whether positive or negative, an  
57  
58  
59  
60



1  
2  
3 592 unexpected outcome attracts more attention, leads to higher levels of emotional arousal and  
4  
5 593 involves higher levels of motor preparation compared to no RPE [Matsumoto and Hikosaka,  
6  
7 594 2009; Maunsell, 2004; Roesch and Olson, 2004]. Consequently, to disentangle these  
8  
9 595 signals, one needs to design tasks in which the level of valence and surprise can  
10  
11 596 independently be controlled and decoupled [Kahnt, 2017; Kahnt and Tobler, 2013] or  
12  
13 597 capitalize on the variability of physiologically-derived responses (i.e. endogenous variability)  
14  
15 598 associated with valence and surprise [Fouragnan et al., 2015; Fouragnan et al., 2017;  
16  
17 599 Pisauro et al., 2017].

18  
19 600

20  
21 601 It is important to note that the problem of collinearity and functional specificity of some  
22  
23 602 brain regions is already present in single studies, it will inevitably be carried over to studies  
24  
25 603 performing conjunction meta-analyses. Virtually every experimental design engages a large  
26  
27 604 number of cognitive operations and, thereby, activates functional neural networks that may  
28  
29 605 be irrelevant to a particular regressor (psychological construct) of interest. For example in  
30  
31 606 our study, regions related to outcome value and surprise might share variance with outcome  
32  
33 607 confidence [Gherman and Philiastides, 2015; Gherman and Philiastides, 2017; Lebreton et  
34  
35 608 al., 2015; Philiastides et al., 2014]. Despite this general limitation and the difficulty of  
36  
37 609 interpreting conjunction results, aggregating results across a large number of experiments  
38  
39 610 allows one to expose convergence of findings across studies and increasing the  
40  
41 611 generalizability of the conclusions. In particular, this meta-analysis, capitalizing on both  
42  
43 612 individual maps of activations as well as contrasts between different outcome components,  
44  
45 613 points to a distributed encoding of valence and surprise, with potentially distinct functional  
46  
47 614 roles.

48  
49 615

### 616 **Temporally specific components of RPE processing**

51  
52 617

53  
54 618 The presence of separate RPE-related neural systems raises the question of how these  
55  
56 619 systems unfold in time. Capitalizing on the high temporal resolution of EEG, three recent  
57  
58  
59  
60

1  
2  
3 620 studies using simultaneous EEG-fMRI have started to shed light on the spatiotemporal  
4  
5 621 characterisation of the RPE components. First, these studies have revealed two temporally  
6  
7 622 specific EEG components discriminating between positive and negative RPEs peaking  
8  
9 623 around 220ms and 300ms respectively, largely consistent with the timing of the feedback-  
10  
11 624 related negativity and feedback-related positivity ERP components [Cohen et al., 2007;  
12  
13 625 Hajcak et al., 2006; Yeung and Sanfey, 2004]. Additionally, the studies also revealed a late  
14  
15 626 unsigned RPE component which overlaps temporally with the late valence signal  
16  
17 627 [Philiastides et al., 2010b] but appears in a largely separate and distributed neural network  
18  
19 628 [Fouragnan et al., 2017].

20  
21 629

22  
23 630 Based on these previous studies and the current meta-analysis, we propose that the early  
24  
25 631 and late EEG valence components might reflect the separate contributions of the two  
26  
27 632 networks of areas found for the ALE-valence analyses. This proposal assumes that an early  
28  
29 633 network processes mainly negative RPEs in order to initiate a fast alertness response in the  
30  
31 634 presence of negative outcomes. Conversely, a later network – associated with the brain's  
32  
33 635 reward circuitry – is modulated by both positive and negative RPEs, consistent with a role in  
34  
35 636 approach/avoidance learning and value updating [Philiastides et al., 2010a]. We also  
36  
37 637 propose that the surprise network unfolds near simultaneously with the late valence  
38  
39 638 component and thus influences learning through largely distinct spatial representations of  
40  
41 639 the two outcomes signals, which happen to form a composite signal in overlapping areas  
42  
43 640 [Fouragnan et al., 2017].

44  
45 641

#### 46 47 642 **Full representation of a monotonic signed RPE signal**

48  
49 643

50  
51 644 To examine the spatial profile of a true monotonic signed RPE representation in the human  
52  
53 645 brain, we pooled results from fMRI studies, which hypothesized that RPE-like learning is  
54  
55 646 driven by a simultaneous representation of both categorical valence and surprise. These

1  
2  
3 647 fMRI studies are based on the influential assumption that BOLD signal increases  
4  
5 648 monotonically as a function of signed RPE, as illustrated in pattern C (Fig. 1), equivalent to  
6  
7 649 the teaching signal that is predicted in the Rescorla–Wagner model of RL [Rescorla and  
8  
9 650 Wagner, 1972]. Additionally, we combined the valence and surprise networks and  
10  
11 651 subsequently compared it with the signed RPE to test the requirement that the signed RPE  
12  
13 652 simultaneously encodes both components. This conjunction analysis revealed that the only  
14  
15 653 brain region that seems to encode a true monotonic signal is the STR in the basal ganglia,  
16  
17 654 which could explain why such a signal is not tractable with EEG recordings as highlighted  
18  
19 655 earlier. This result confirms the long standing view that the BOLD activity in STR mirrors the  
20  
21 656 dopaminergic signalling of the mesolimbic neurons [Delgado et al., 2000; Haber et al., 1995;  
22  
23 657 O'Doherty et al., 2004; Pagnoni et al., 2002] that fully encode the RL prediction error signal  
24  
25 658 of the Rescorla-Wagner rule [Ikemoto, 2007; Schultz et al., 1992].

26  
27 659

28  
29 660 Nonetheless, the ALE contrast analyses between valence (the positive correlation with  
30  
31 661 pattern A (ii)) and signed RPE revealed no significant activation, whereas the reverse  
32  
33 662 contrast revealed a denser cluster of activity in vmPFC for valence than signed RPE. Given  
34  
35 663 the evidence presented above that the signed RPE may only be encoded in the STR, we  
36  
37 664 suggest that this result may arise due to collinearities between valence and signed RPE or  
38  
39 665 surprise and signed RPE. More precisely, a parametric predictor for signed RPE would be  
40  
41 666 positively correlated with the contrast positive > negative outcomes whereas the signed RPE  
42  
43 667 and surprise would be perfectly correlated in the positive (appetitive) domain.

44  
45 668

## 46 669 **Conclusion**

47  
48  
49 670

50  
51 671 In conclusion, the current meta-analysis points to a framework whereby heterogeneous  
52  
53 672 signals are involved in RPE processing. The proposal of a temporally distinct and spatially  
54  
55 673 distributed representation of valence and surprise is open to debate and many questions  
56  
57 674 remain about how these signals interact and how they correspond to the computations made

1  
2  
3 675 in the brain. For example, it is currently unclear whether valence and surprise encoding  
4  
5 676 occur before the computation of the signed RPE, or whether these three computations are  
6  
7 677 performed in parallel. Nevertheless the taxonomy proposed is conceptually useful because it  
8  
9 678 breaks down the learning and valuation processes into testable components and organizes  
10  
11 679 the RPE literature in terms of the computations that are potentially involved. It will require  
12  
13 680 additional experiments to validate the current proposal and to better understand the  
14  
15 681 complexity of RPE processing.

16  
17 682

18  
19  
20  
21  
22  
23  
24  
25  
26  
27  
28  
29  
30  
31  
32  
33  
34  
35  
36  
37  
38  
39  
40  
41  
42  
43  
44  
45  
46  
47  
48  
49  
50  
51  
52  
53  
54  
55  
56  
57  
58  
59  
60

For Peer Review

683 **References**

- 684 Abler B, Walter H, Erk S, Kammerer H, Spitzer M (2006): Prediction error as a linear function  
685 of reward probability is coded in human nucleus accumbens. *NeuroImage* 31:790–  
686 795.
- 687 Allen M, Fardo F, Dietz MJ, Hillebrandt H, Friston KJ, Rees G, Roepstorff A (2016): Anterior  
688 insula coordinates hierarchical processing of tactile mismatch responses.  
689 *NeuroImage* 127:34–43.
- 690 Amado C, Hermann P, Kovács P, Grotheer M, Vidnyánszky Z, Kovács G (2016): The  
691 contribution of surprise to the prediction based modulation of fMRI responses.  
692 *Neuropsychologia* 84:105–112.
- 693 Amiez C, Sallet J, Procyk E, Petrides M (2012): Modulation of feedback related activity in the  
694 rostral anterior cingulate cortex during trial and error exploration. *NeuroImage*  
695 63:1078–1090.
- 696 Aron AR, Shohamy D, Clark J, Myers C, Gluck MA, Poldrack RA (2004): Human Midbrain  
697 Sensitivity to Cognitive Feedback and Uncertainty During Classification Learning. *J*  
698 *Neurophysiol* 92:1144–1152.
- 699 Bartra O, McGuire JT, Kable JW (2013): The valuation system: a coordinate-based meta-  
700 analysis of BOLD fMRI experiments examining neural correlates of subjective value.  
701 *NeuroImage* 76:412–427.
- 702 Behrens TEJ, Woolrich MW, Walton ME, Rushworth MFS (2007): Learning the value of  
703 information in an uncertain world. *Nat Neurosci* 10:1214–1221.
- 704 Bickel WK, Pitcock JA, Yi R, Angtuaco EJC (2009): Congruence of BOLD Response across  
705 Intertemporal Choice Conditions: Fictive and Real Money Gains and Losses. *J*  
706 *Neurosci* 29:8839–8846.
- 707 Boll S, Gamer M, Gluth S, Finsterbusch J, Büchel C (2013): Separate amygdala subregions  
708 signal surprise and predictiveness during associative fear learning in humans. *Eur J*  
709 *Neurosci* 37:758–767.
- 710 van den Bos W, Cohen MX, Kahnt T, Crone EA (2012): Striatum-medial prefrontal cortex  
711 connectivity predicts developmental changes in reinforcement learning. *Cereb*  
712 *Cortex N Y N* 1991 22:1247–1255.
- 713 Boureau Y-L, Dayan P (2011): Opponency Revisited: Competition and Cooperation Between  
714 Dopamine and Serotonin. *Neuropsychopharmacology* 36:74–97.
- 715 Brischoux F, Chakraborty S, Brierley DI, Ungless MA (2009): Phasic excitation of dopamine  
716 neurons in ventral VTA by noxious stimuli. *Proc Natl Acad Sci U S A* 106:4894–4899.
- 717 Browning M, Holmes EA, Murphy SE, Goodwin GM, Harmer CJ (2010): Lateral Prefrontal  
718 Cortex Mediates the Cognitive Modification of Attentional Bias. *Biol Psychiatry*  
719 67:919–925.
- 720 de Bruijn E, de Lange F, Cramon D, Ullsperger M (2009): When Errors Are Rewarding. *J*  
721 *Neurosci Off J Soc Neurosci* 29:12183–6.
- 722 Canessa N, Crespi C, Motterlini M, Baud-Bovy G, Chierchia G, Pantaleo G, Tettamanti M,  
723 Cappa SF (2013): The Functional and Structural Neural Basis of Individual Differences  
724 in Loss Aversion. *J Neurosci* 33:14307–14317.
- 725 Chumbley JR, Burke CJ, Stephan KE, Friston KJ, Tobler PN, Fehr E (2014): Surprise beyond  
726 prediction error. *Hum Brain Mapp* 35:4805–4814.

- 1  
2  
3 727 Cohen MX, Elger CE, Ranganath C (2007): Reward Expectation Modulates Feedback-Related  
4 728 Negativity and EEG Spectra. *NeuroImage* 35:968–978.
- 5 729 Cohen MX, Ranganath C (2007): Reinforcement Learning Signals Predict Future Decisions. *J*  
6 730 *Neurosci* 27:371–378.
- 7 731 Collins AGE, Frank MJ (2016): Surprise! Dopamine signals mix action, value and error. *Nat*  
8 732 *Neurosci* 19:3–5.
- 9 733 Cools R, Nakamura K, Daw ND (2011): Serotonin and Dopamine: Unifying Affective,  
10 734 Activational, and Decision Functions. *Neuropsychopharmacology* 36:98–113.
- 11 735 Courville AC, Daw ND, Touretzky DS (2006): Bayesian theories of conditioning in a changing  
12 736 world. *Trends Cogn Sci* 10:294–300.
- 13 737 Daniel R, Wagner G, Koch K, Reichenbach JR, Sauer H, Schlösser RGM (2011): Assessing the  
14 738 neural basis of uncertainty in perceptual category learning through varying levels of  
15 739 distortion. *J Cogn Neurosci* 23:1781–1793.
- 16 740 D’Ardenne K, McClure SM, Nystrom LE, Cohen JD (2008): BOLD responses reflecting  
17 741 dopaminergic signals in the human ventral tegmental area. *Science* 319:1264–1267.
- 18 742 Daw ND, Niv Y, Dayan P (2005): Uncertainty-based competition between prefrontal and  
19 743 dorsolateral striatal systems for behavioral control. *Nat Neurosci* 8:1704–1711.
- 20 744 Daw ND, Gershman SJ, Seymour B, Dayan P, Dolan RJ (2011): Model-Based Influences on  
21 745 Humans’ Choices and Striatal Prediction Errors. *Neuron* 69:1204–1215.
- 22 746 Dayan P, Balleine BW (2002): Reward, motivation, and reinforcement learning. *Neuron*  
23 747 36:285–298.
- 24 748 Delgado MR, Nystrom LE, Fissell C, Noll DC, Fiez JA (2000): Tracking the Hemodynamic  
25 749 Responses to Reward and Punishment in the Striatum. *J Neurophysiol* 84:3072–  
26 750 3077.
- 27 751 Delgado MR (2007): Reward-Related Responses in the Human Striatum. *Ann N Y Acad Sci*  
28 752 1104:70–88.
- 29 753 Demos KE, Heatherton TF, Kelley WM (2012): Individual Differences in Nucleus Accumbens  
30 754 Activity to Food and Sexual Images Predict Weight Gain and Sexual Behavior. *J*  
31 755 *Neurosci* 32:5549–5552.
- 32 756 Diederer KJM, Ziauddeen H, Vestergaard MD, Spencer T, Schultz W, Fletcher PC (2017):  
33 757 Dopamine Modulates Adaptive Prediction Error Coding in the Human Midbrain and  
34 758 Striatum. *J Neurosci Off J Soc Neurosci* 37:1708–1720.
- 35 759 Diuk C, Tsai K, Wallis J, Botvinick M, Niv Y (2013): Hierarchical Learning Induces Two  
36 760 Simultaneous, But Separable, Prediction Errors in Human Basal Ganglia. *J Neurosci*  
37 761 33:5797–5805.
- 38 762 Doya K, Samejima K, Katagiri K, Kawato M (2002): Multiple model-based reinforcement  
39 763 learning. *Neural Comput* 14:1347–1369.
- 40 764 Dreher J-C (2013): Neural coding of computational factors affecting decision making. *Prog*  
41 765 *Brain Res* 202:289–320.
- 42 766 van Duijvenvoorde ACK, Op de Macks ZA, Overgaauw S, Gunther Moor B, Dahl RE, Crone EA  
43 767 (2014): A cross-sectional and longitudinal analysis of reward-related brain activation:  
44 768 Effects of age, pubertal stage, and reward sensitivity. *Brain Cogn* 89:3–14.
- 45 769 Dunne S, D’Souza A, O’Doherty JP (2016): The involvement of model-based but not model-  
46 770 free learning signals during observational reward learning in the absence of choice. *J*  
47 771 *Neurophysiol* 115:3195–3203.
- 48 772 Eickhoff SB, Etkin A (2016): Going Beyond Finding the “Lesion”: A Path for Maturation of  
49 773 Neuroimaging. *Am J Psychiatry* 173:302–303.

- 1  
2  
3 774 Eickhoff SB, Laird AR, Fox PM, Lancaster JL, Fox PT (2017): Implementation errors in the  
4 775 GingerALE Software: Description and recommendations. *Hum Brain Mapp* 38:7–11.  
5 776 Eickhoff SB, Laird AR, Grefkes C, Wang LE, Zilles K, Fox PT (2009): Coordinate-based  
6 777 activation likelihood estimation meta-analysis of neuroimaging data: a random-  
7 778 effects approach based on empirical estimates of spatial uncertainty. *Hum Brain*  
8 779 *Mapp* 30:2907–2926.
- 10 780 Elliot AJ (2006): The Hierarchical Model of Approach-Avoidance Motivation. *Motiv Emot*  
11 781 30:111–116.
- 12 782 Elliott R, Friston KJ, Dolan RJ (2000): Dissociable neural responses in human reward systems.  
13 783 *J Neurosci Off J Soc Neurosci* 20:6159–6165.
- 14 784 Elward RL, Vilberg KL, Rugg MD (2015): Motivated Memories: Effects of Reward and  
15 785 Recollection in the Core Recollection Network and Beyond. *Cereb Cortex* 25:3159–  
16 786 3166.
- 18 787 Ernst M, Nelson EE, McClure EB, Monk CS, Munson S, Eshel N, Zarahn E, Leibenluft E,  
19 788 Zametkin A, Towbin K, Blair J, Charney D, Pine DS (2004): Choice selection and  
20 789 reward anticipation: an fMRI study. *Neuropsychologia* 42:1585–1597.
- 21 790 Ferdinand NK, Opitz B (2014): Different aspects of performance feedback engage different  
22 791 brain areas: Disentangling valence and expectancy in feedback processing. *Sci Rep*  
23 792 4:srep05986.
- 25 793 Fiorillo CD (2013): Two Dimensions of Value: Dopamine Neurons Represent Reward But Not  
26 794 Aversiveness. *Science* 341:546–549.
- 27 795 Fiorillo CD, Tobler PN, Schultz W (2003): Discrete Coding of Reward Probability and  
28 796 Uncertainty by Dopamine Neurons. *Science* 299:1898–1902.
- 29 797 Forster SE, Brown JW (2011): Medial prefrontal cortex predicts and evaluates the timing of  
30 798 action outcomes. *NeuroImage* 55:253–265.
- 32 799 Fouragnan E, Chierchia G, Greiner S, Neveu R, Avesani P, Coricelli G (2013): Reputational  
33 800 Priors Magnify Striatal Responses to Violations of Trust. *J Neurosci* 33:3602–3611.
- 34 801 Fouragnan E, Queirazza F, Retzler C, Mullinger K, Philiastides M (2017): Spatiotemporal  
35 802 neural characterization of prediction error valence and surprise during reward  
36 803 learning in humans. *Sci Rep*. <https://www.nature.com/srep/>.
- 38 804 Fouragnan E, Retzler C, Mullinger K, Philiastides MG (2015): Two spatiotemporally distinct  
39 805 value systems shape reward-based learning in the human brain. *Nat Commun*  
40 806 6:8107.
- 41 807 Frank MJ, Seeberger LC, O'reilly RC (2004): By carrot or by stick: cognitive reinforcement  
42 808 learning in parkinsonism. *Science* 306:1940–1943.
- 43 809 Friston K (2009): The free-energy principle: a rough guide to the brain? *Trends Cogn Sci*  
44 810 13:293–301.
- 45 811 Friston K, Kilner J, Harrison L (2006): A free energy principle for the brain. *J Physiol Paris*  
46 812 100:70–87.
- 48 813 Fujiwara J, Tobler PN, Taira M, Iijima T, Tsutsui K-I (2009): Segregated and integrated coding  
49 814 of reward and punishment in the cingulate cortex. *J Neurophysiol* 101:3284–3293.
- 50 815 Garrison J, Erdeniz B, Done J (2013): Prediction error in reinforcement learning: A meta-  
51 816 analysis of neuroimaging studies. *Neurosci Biobehav Rev* 37:1297–1310.
- 52 817 Gherman S, Philiastides MG (2015): Neural representations of confidence emerge from the  
53 818 process of decision formation during perceptual choices. *NeuroImage* 106:134–143.
- 54 819 Gherman S, Philiastides MG (2017): Human VMPFC encodes early signatures of confidence  
56 820 in perceptual decisions. *bioRxiv:224337*.

- 1  
2  
3 821 Gläscher J, Daw N, Dayan P, O'Doherty JP (2010): States versus rewards: dissociable neural  
4 822 prediction error signals underlying model-based and model-free reinforcement  
5 823 learning. *Neuron* 66:585–595.
- 6 824 Gläscher J, Hampton AN, O'Doherty JP (2009): Determining a Role for Ventromedial  
7 825 Prefrontal Cortex in Encoding Action-Based Value Signals During Reward-Related  
8 826 Decision Making. *Cereb Cortex* 19:483–495.
- 9 827 Gray JA, McNaughton N (2003): *The Neuropsychology of Anxiety: An Enquiry Into the*  
10 828 *Function of the Septo-hippocampal System*. Oxford University Press.
- 11 829 Guitart-Masip M, Huys QJM, Fuentemilla L, Dayan P, Duzel E, Dolan RJ (2012): Go and no-go  
12 830 learning in reward and punishment: interactions between affect and effect.  
13 831 *NeuroImage* 62:154–166.
- 14 832 Guo R, Böhmer W, Hebart M, Chien S, Sommer T, Obermayer K, Gläscher J (2016):  
15 833 Interaction of Instrumental and Goal-Directed Learning Modulates Prediction Error  
16 834 Representations in the Ventral Striatum. *J Neurosci* 36:12650–12660.
- 17 835 Haber SN, Kunishio K, Mizobuchi M, Lynd-Balta E (1995): The orbital and medial prefrontal  
18 836 circuit through the primate basal ganglia. *J Neurosci Off J Soc Neurosci* 15:4851–  
19 837 4867.
- 20 838 Hajcak G, Moser JS, Holroyd CB, Simons RF (2006): The feedback-related negativity reflects  
21 839 the binary evaluation of good versus bad outcomes. *Biol Psychol* 71:148–154.
- 22 840 Hall G, Pearce JM (1979): Latent inhibition of a CS during CS-US pairings. *J Exp Psychol Anim*  
23 841 *Behav Process* 5:31–42.
- 24 842 Hare TA, O'Doherty J, Camerer CF, Schultz W, Rangel A (2008): Dissociating the Role of the  
25 843 Orbitofrontal Cortex and the Striatum in the Computation of Goal Values and  
26 844 Prediction Errors. *J Neurosci* 28:5623–5630.
- 27 845 Haruno M, Kuroda T, Doya K, Toyama K, Kimura M, Samejima K, Imamizu H, Kawato M  
28 846 (2004): A neural correlate of reward-based behavioral learning in caudate nucleus: a  
29 847 functional magnetic resonance imaging study of a stochastic decision task. *J Neurosci*  
30 848 *Off J Soc Neurosci* 24:1660–1665.
- 31 849 Häusler AN, Oroz Artigas S, Trautner P, Weber B (2016): Gain- and Loss-Related Brain  
32 850 Activation Are Associated with Information Search Differences in Risky Gambles: An  
33 851 fMRI and Eye-Tracking Study. *eNeuro* 3.  
34 852 <https://www.ncbi.nlm.nih.gov/pmc/articles/PMC5032244/>.
- 35 853 Hayden BY, Heilbronner SR, Pearson JM, Platt ML (2011): Surprise Signals in Anterior  
36 854 Cingulate Cortex: Neuronal Encoding of Unsigned Reward Prediction Errors Driving  
37 855 Adjustment in Behavior. *J Neurosci* 31:4178–4187.
- 38 856 Hester R, Barre N, Murphy K, Silk TJ, Mattingley JB (2008): Human Medial Frontal Cortex  
39 857 Activity Predicts Learning from Errors. *Cereb Cortex* 18:1933–1940.
- 40 858 Hester R, Murphy K, Brown FL, Skilleter AJ (2010): Punishing an Error Improves Learning: The  
41 859 Influence of Punishment Magnitude on Error-Related Neural Activity and Subsequent  
42 860 Learning. *J Neurosci* 30:15600–15607.
- 43 861 Huettel SA, Stowe CJ, Gordon EM, Warner BT, Platt ML (2006): Neural signatures of  
44 862 economic preferences for risk and ambiguity. *Neuron* 49:765–775.
- 45 863 Ide JS, Shenoy P, Yu AJ, Li CR (2013): Bayesian Prediction and Evaluation in the Anterior  
46 864 Cingulate Cortex. *J Neurosci* 33:2039–2047.
- 47 865 Iglesias S, Mathys C, Brodersen KH, Kasper L, Piccirelli M, den Ouden HEM, Stephan KE  
48 866 (2013): Hierarchical Prediction Errors in Midbrain and Basal Forebrain during Sensory  
49 867 Learning. *Neuron* 80:519–530.



- 1  
2  
3 868 Ikemoto S (2007): Dopamine reward circuitry: Two projection systems from the ventral  
4 869 midbrain to the nucleus accumbens–olfactory tubercle complex. *Brain Res Rev*  
5 870 56:27–78.
- 6 871 Jenkinson M, Bannister P, Brady M, Smith S (2002): Improved optimization for the robust  
7 872 and accurate linear registration and motion correction of brain images. *NeuroImage*  
8 873 17:825–841.
- 9 874 Jensen J, Smith AJ, Willeit M, Crawley AP, Mikulis DJ, Vitcu I, Kapur S (2007): Separate brain  
10 875 regions code for salience vs. valence during reward prediction in humans. *Hum Brain*  
11 876 *Mapp* 28:294–302.
- 12 877 Jocham G, Brodersen KH, Constantinescu AO, Kahn MC, Ianni AM, Walton ME, Rushworth  
13 878 MFS, Behrens TEJ (2016): Reward-Guided Learning with and without Causal  
14 879 Attribution. *Neuron* 90:177–190.
- 15 880 Kaelbling LP, Littman ML, Moore AW (1996): Reinforcement Learning: A Survey.  
16 881 arXiv:cs/9605103. <http://arxiv.org/abs/cs/9605103>.
- 17 882 Kahnt T (2017): A decade of decoding reward-related fMRI signals and where we go from  
18 883 here. *NeuroImage*.  
19 884 <http://www.sciencedirect.com/science/article/pii/S1053811917304688>.
- 20 885 Kahnt T, Heinzle J, Park SQ, Haynes J-D (2010): The neural code of reward anticipation in  
21 886 human orbitofrontal cortex. *Proc Natl Acad Sci* 107:6010–6015.
- 22 887 Kahnt T, Tobler PN (2013): Salience Signals in the Right Temporoparietal Junction Facilitate  
23 888 Value-Based Decisions. *J Neurosci* 33:863–869.
- 24 889 Katahira K, Matsuda Y-T, Fujimura T, Ueno K, Asamizuya T, Suzuki C, Cheng K, Okanoya K,  
25 890 Okada M (2015): Neural basis of decision making guided by emotional outcomes. *J*  
26 891 *Neurophysiol* 113:3056–3068.
- 27 892 Klein-Flügge MC, Hunt LT, Bach DR, Dolan RJ, Behrens TEJ (2011): Dissociable reward and  
28 893 timing signals in human midbrain and ventral striatum. *Neuron* 72:654–664.
- 29 894 Knutson B, Adams CM, Fong GW, Hommer D (2001): Anticipation of increasing monetary  
30 895 reward selectively recruits nucleus accumbens. *J Neurosci Off J Soc Neurosci*  
31 896 21:RC159.
- 32 897 Knutson B, Westdorp A, Kaiser E, Hommer D (2000): FMRI visualization of brain activity  
33 898 during a monetary incentive delay task. *NeuroImage* 12:20–27.
- 34 899 Koch K, Schachtzabel C, Wagner G, Reichenbach JR, Sauer H, Schlösser R (2008): The neural  
35 900 correlates of reward-related trial-and-error learning: An fMRI study with a  
36 901 probabilistic learning task. *Learn Mem* 15:728–732.
- 37 902 Kolling N, Behrens TEJ, Mars RB, Rushworth MFS (2012): Neural Mechanisms of Foraging.  
38 903 *Science* 336:95–98.
- 39 904 Kotz SA, Dengler R, Wittfoth M (2015): Valence-specific conflict moderation in the dorso-  
40 905 medial PFC and the caudate head in emotional speech. *Soc Cogn Affect Neurosci*  
41 906 10:165–171.
- 42 907 Kurniawan IT, Guitart-Masip M, Dayan P, Dolan RJ (2013): Effort and valuation in the brain:  
43 908 the effects of anticipation and execution. *J Neurosci Off J Soc Neurosci* 33:6160–  
44 909 6169.
- 45 910 Laird AR, Fox PM, Price CJ, Glahn DC, Uecker AM, Lancaster JL, Turkeltaub PE, Kochunov P,  
46 911 Fox PT (2005): ALE meta-analysis: controlling the false discovery rate and performing  
47 912 statistical contrasts. *Hum Brain Mapp* 25:155–164.
- 48 913 Lebreton M, Abitbol R, Daunizeau J, Pessiglione M (2015): Automatic integration of  
49 914 confidence in the brain valuation signal. *Nat Neurosci* 18:1159–1167.

- 1  
2  
3 915 Leknes S, Lee M, Berna C, Andersson J, Tracey I (2011): Relief as a Reward: Hedonic and  
4 916 Neural Responses to Safety from Pain. *PLOS ONE* 6:e17870.
- 5 917 Leong YC, Radulescu A, Daniel R, DeWoskin V, Niv Y (2017): Dynamic Interaction between  
6 918 Reinforcement Learning and Attention in Multidimensional Environments. *Neuron*  
7 919 93:451–463.
- 8 920 Li J, Daw ND (2011): Signals in human striatum are appropriate for policy update rather than  
9 921 value prediction. *J Neurosci Off J Soc Neurosci* 31:5504–5511.
- 10 922 Li J, Zhang Y (2006): Prediction error method-based second-order structural identification  
11 923 algorithm in stochastic state space formulation. *Earthq Eng Struct Dyn* 35:761–779.
- 12 924 Lin A, Adolphs R, Rangel A (2012): Social and monetary reward learning engage overlapping  
13 925 neural substrates. *Soc Cogn Affect Neurosci* 7:274–281.
- 14 926 Litt A, Plassmann H, Shiv B, Rangel A (2011): Dissociating valuation and saliency signals  
15 927 during decision-making. *Cereb Cortex N Y N 1991* 21:95–102.
- 16 928 Liu X, Hairston J, Schrier M, Fan J (2011): Common and distinct networks underlying reward  
17 929 valence and processing stages: a meta-analysis of functional neuroimaging studies.  
18 930 *Neurosci Biobehav Rev* 35:1219–1236.
- 19 931 Losecaat Vermeer A, Boksem M, G Sanfey A (2014): Neural mechanisms underlying context-  
20 932 dependent shifts in risk preferences. *NeuroImage* 103.
- 21 933 Luking KR, Luby JL, Barch DM (2014): Kids, candy, brain and behavior: Age differences in  
22 934 responses to candy gains and losses. *Dev Cogn Neurosci* 9:82–92.
- 23 935 Manza P, Hu S, Ide JS, Farr OM, Zhang S, Leung H-C, Li CR (2016): The effects of  
24 936 methylphenidate on cerebral responses to conflict anticipation and unsigned  
25 937 prediction error in a stop-signal task. *J Psychopharmacol Oxf Engl* 30:283–293.
- 26 938 Marsh R, Hao X, Xu D, Wang Z, Duan Y, Liu J, Kangarlu A, Martinez D, Garcia F, Tau GZ, Yu S,  
27 939 Packard MG, Peterson BS (2010): A virtual reality-based fMRI study of reward-based  
28 940 spatial learning. *Neuropsychologia* 48:2912–2921.
- 29 941 Mathys CD, Lomakina EI, Daunizeau J, Iglesias S, Brodersen KH, Friston KJ, Stephan KE  
30 942 (2014): Uncertainty in perception and the Hierarchical Gaussian Filter. *Front Hum*  
31 943 *Neurosci* 8. <http://journal.frontiersin.org/article/10.3389/fnhum.2014.00825/full>.
- 32 944 Matsumoto M, Hikosaka O (2009): Two types of dopamine neuron distinctly convey positive  
33 945 and negative motivational signals. *Nature* 459:837–841.
- 34 946 Mattfeld AT, Gluck MA, Stark CEL (2011): Functional specialization within the striatum along  
35 947 both the dorsal/ventral and anterior/posterior axes during associative learning via  
36 948 reward and punishment. *Learn Mem Cold Spring Harb N* 18:703–711.
- 37 949 Maunsell JHR (2004): Neuronal representations of cognitive state: reward or attention?  
38 950 *Trends Cogn Sci* 8:261–265.
- 39 951 McClure SM, Berns GS, Montague PR (2003): Temporal prediction errors in a passive  
40 952 learning task activate human striatum. *Neuron* 38:339–346.
- 41 953 Menon V, Levitin DJ (2005): The rewards of music listening: response and physiological  
42 954 connectivity of the mesolimbic system. *NeuroImage* 28:175–184.
- 43 955 Metereau E, Dreher J-C (2013): Cerebral correlates of salient prediction error for different  
44 956 rewards and punishments. *Cereb Cortex N Y N 1991* 23:477–487.
- 45 957 Metereau E, Dreher J-C (2015): The medial orbitofrontal cortex encodes a general unsigned  
46 958 value signal during anticipation of both appetitive and aversive events. *Cortex J*  
47 959 *Devoted Study Nerv Syst Behav* 63:42–54.
- 48 960 Meyniel F, Dehaene S (2017): Brain networks for confidence weighting and hierarchical  
49 961 inference during probabilistic learning. *Proc Natl Acad Sci* 114:E3859–E3868.

1

2

3

4

5

6

7

8

9

10

11

12

13

14

15

16

17

18

19

20

21

22

23

24

25

26

27

28

29

30

31

32

33

34

35

36

37

38

39

40

41

42

43

44

45

46

47

48

49

50

51

52

53

54

55

56

57

58

59

60

- 962 Middlebrooks PG, Sommer MA (2012): Neuronal correlates of metacognition in primate  
963 frontal cortex. *Neuron* 75:517–530.
- 964 Montague PR, Dayan P, Sejnowski TJ (1996): A framework for mesencephalic dopamine  
965 systems based on predictive Hebbian learning. *J Neurosci Off J Soc Neurosci*  
966 16:1936–1947.
- 967 Morrens J (2014): Dopamine neurons coding prediction errors in reward space, but not in  
968 aversive space: a matter of location? *J Neurophysiol* 112:1021–1024.
- 969 Nassar MR, Rumsey KM, Wilson RC, Parikh K, Heasley B, Gold JI (2012): Rational regulation of  
970 learning dynamics by pupil-linked arousal systems. *Nat Neurosci* 15:1040–1046.
- 971 Nieuwenhuis S, Slagter HA, von Geusau NJA, Heslenfeld DJ, Holroyd CB (2005): Knowing  
972 good from bad: differential activation of human cortical areas by positive and  
973 negative outcomes. *Eur J Neurosci* 21:3161–3168.
- 974 Niv Y, Daniel R, Geana A, Gershman SJ, Leong YC, Radulescu A, Wilson RC (2015):  
975 Reinforcement Learning in Multidimensional Environments Relies on Attention  
976 Mechanisms. *J Neurosci* 35:8145–8157.
- 977 Noonan MP, Mars RB, Rushworth MFS (2011): Distinct roles of three frontal cortical areas in  
978 reward-guided behavior. *J Neurosci Off J Soc Neurosci* 31:14399–14412.
- 979 O’Doherty J, Kringelbach ML, Rolls ET, Hornak J, Andrews C (2001): Abstract reward and  
980 punishment representations in the human orbitofrontal cortex. *Nat Neurosci* 4:95–  
981 102.
- 982 O’Doherty J, Critchley H, Deichmann R, Dolan RJ (2003): Dissociating valence of outcome  
983 from behavioral control in human orbital and ventral prefrontal cortices. *J Neurosci*  
984 *Off J Soc Neurosci* 23:7931–7939.
- 985 O’Doherty J, Dayan P, Schultz J, Deichmann R, Friston K, Dolan RJ (2004): Dissociable Roles  
986 of Ventral and Dorsal Striatum in Instrumental Conditioning. *Science* 304:452–454.
- 987 O’Doherty JP, Hampton A, Kim H (2007): Model-Based fMRI and Its Application to Reward  
988 Learning and Decision Making. *Ann N Y Acad Sci* 1104:35–53.
- 989 Oostenveld R, Fries P, Maris E, Schoffelen J-M (2011): FieldTrip: Open Source Software for  
990 Advanced Analysis of MEG, EEG, and Invasive Electrophysiological Data. Research  
991 article. *Computational Intelligence and Neuroscience*.  
992 <https://www.hindawi.com/journals/cin/2011/156869/>.
- 993 O’Reilly JX, Schüffelgen U, Cuell SF, Behrens TEJ, Mars RB, Rushworth MFS (2013):  
994 Dissociable effects of surprise and model update in parietal and anterior cingulate  
995 cortex. *Proc Natl Acad Sci* 110:E3660–E3669.
- 996 den Ouden HEM, Kok P, de Lange FP (2012): How Prediction Errors Shape Perception,  
997 Attention, and Motivation. *Front Psychol* 3.  
998 <http://www.ncbi.nlm.nih.gov/pmc/articles/PMC3518876/>.
- 999 Pagnoni G, Zink CF, Montague PR, Berns GS (2002): Activity in human ventral striatum  
1000 locked to errors of reward prediction. *Nat Neurosci* 5:97–98.
- 1001 Paschke LM, Walter H, Steimke R, Ludwig VU, Gaschler R, Schubert T, Stelzel C (2015):  
1002 Motivation by potential gains and losses affects control processes via different  
1003 mechanisms in the attentional network. *NeuroImage* 111:549–561.
- 1004 Pearce JM, Hall G (1980): A model for Pavlovian learning: Variations in the effectiveness of  
1005 conditioned but not of unconditioned stimuli. *Psychol Rev* 87:532–552.
- 1006 Pessiglione M, Petrovic P, Daunizeau J, Palminteri S, Dolan RJ, Frith CD (2008): Subliminal  
1007 instrumental conditioning demonstrated in the human brain. *Neuron* 59:561–567.

- 1  
2  
3 1008 Pessiglione M, Seymour B, Flandin G, Dolan RJ, Frith CD (2006): Dopamine-dependent  
4 1009 prediction errors underpin reward-seeking behaviour in humans. *Nature* 442:1042–  
5 1010 1045.
- 6 1011 Philiastides MG, Biele G, Heekeren HR (2010a): A mechanistic account of value computation  
7 1012 in the human brain. *Proc Natl Acad Sci U S A* 107:9430–9435.
- 8 1013 Philiastides MG, Biele G, Vavatzanidis N, Kazzner P, Heekeren HR (2010b): Temporal dynamics  
9 1014 of prediction error processing during reward-based decision making. *NeuroImage*  
10 1015 53:221–232.
- 11 1016 Philiastides MG, Heekeren HR, Sajda P (2014): Human Scalp Potentials Reflect a Mixture of  
12 1017 Decision-Related Signals during Perceptual Choices. *J Neurosci* 34:16877–16889.
- 13 1018 Pisauro A, Fouragnan E, Retzler C, Philiastides M (2017): Neural correlates of evidence  
14 1019 accumulation during value-based decisions revealed via simultaneous EEG-fMRI. *Nat*  
15 1020 *Commun.* <http://eprints.hud.ac.uk/31834/>.
- 16 1021 Poudel GR, Innes CRH, Jones RD (2013): Distinct neural correlates of time-on-task and  
17 1022 transient errors during a visuomotor tracking task after sleep restriction.  
18 1023 *NeuroImage* 77:105–113.
- 19 1024 Preuschoff K, Quartz SR, Bossaerts P (2008): Human Insula Activation Reflects Risk  
20 1025 Prediction Errors As Well As Risk. *J Neurosci* 28:2745–2752.
- 21 1026 Queirazza F, Fouragnan E, Steele JD, Cavanagh J, Philiastides M (2017): Dorsomedial  
22 1027 prefrontal cortex activity during reinforcement learning discriminates response to  
23 1028 Cognitive Behavioural Therapy in depression. *bioRxiv:224410*.
- 24 1029 R Garrison J, Done J, S Simons J (2017): Interpretation of published meta-analytical studies  
25 1030 affected by implementation errors in the GingerALE software.
- 26 1031 Rescorla R, Wagner A (1972): A theory of Pavlovian conditioning: Variations in the  
27 1032 effectiveness of reinforcement and nonreinforcement. In: Black, A, Prokasy, W,  
28 1033 editors. *Classical Conditioning II: Current Research and Theory*. Appleton-Century-  
29 1034 Crofts. pp 64–99.
- 30 1035 Ribas-Fernandes JFF, Solway A, Diuk C, McGuire JT, Barto AG, Niv Y, Botvinick MM (2011): A  
31 1036 neural signature of hierarchical reinforcement learning. *Neuron* 71:370–379.
- 32 1037 Rodriguez PF (2009): Stimulus-outcome learnability differentially activates anterior cingulate  
33 1038 and hippocampus at feedback processing. *Learn Mem Cold Spring Harb N* 16:324–  
34 1039 331.
- 35 1040 Roesch MR, Olson CR (2004): Neuronal Activity Related to Reward Value and Motivation in  
36 1041 Primate Frontal Cortex. *Science* 304:307–310.
- 37 1042 Rohe T, Noppeney U (2015): Cortical Hierarchies Perform Bayesian Causal Inference in  
38 1043 Multisensory Perception. *PLOS Biol* 13:e1002073.
- 39 1044 Rohe T, Weber B, Fliessbach K (2012): Dissociation of BOLD responses to reward prediction  
40 1045 errors and reward receipt by a model comparison. *Eur J Neurosci* 36:2376–2382.
- 41 1046 Rolls ET, Grabenhorst F, Parris BA (2008): Warm pleasant feelings in the brain. *NeuroImage*  
42 1047 41:1504–1513.
- 43 1048 Rudolf S, Preuschoff K, Weber B (2012): Neural Correlates of Anticipation Risk Reflect Risk  
44 1049 Preferences. *J Neurosci* 32:16683–16692.
- 45 1050 Samson RD, Frank MJ, Fellous J-M (2010): Computational models of reinforcement learning:  
46 1051 the role of dopamine as a reward signal. *Cogn Neurodyn* 4:91–105.
- 47 1052 Sarinopoulos I, Grupe DW, Mackiewicz KL, Herrington JD, Lor M, Steege EE, Nitschke JB  
48 1053 (2010): Uncertainty during anticipation modulates neural responses to aversion in  
49 1054 human insula and amygdala. *Cereb Cortex N Y N* 1991 20:929–940.

- 1  
2  
3 1055 Schlagenhaut F, Rapp MA, Huys QJM, Beck A, Wüstenberg T, Deserno L, Buchholz H-G,  
4 1056 Kalbitzer J, Buchert R, Bauer M, Kienast T, Cumming P, Plotkin M, Kumakura Y, Grace  
5 1057 AA, Dolan RJ, Heinz A (2013): Ventral striatal prediction error signaling is associated  
6 1058 with dopamine synthesis capacity and fluid intelligence. *Hum Brain Mapp* 34:1490–  
7 1059 1499.
- 8 1060 Scholl J, Kolling N, Nelissen N, Wittmann MK, Harmer CJ, Rushworth MFS (2015): The Good,  
9 1061 the Bad, and the Irrelevant: Neural Mechanisms of Learning Real and Hypothetical  
10 1062 Rewards and Effort. *J Neurosci Off J Soc Neurosci* 35:11233–11251.
- 11 1063 Schonberg T, O’Doherty JP, Joel D, Inzelberg R, Segev Y, Daw ND (2010): Selective  
12 1064 impairment of prediction error signaling in human dorsolateral but not ventral  
13 1065 striatum in Parkinson’s disease patients: evidence from a model-based fMRI study.  
14 1066 *NeuroImage* 49:772–781.
- 15 1067 Schultz W, Apicella P, Ljungberg T (1993): Responses of monkey dopamine neurons to  
16 1068 reward and conditioned stimuli during successive steps of learning a delayed  
17 1069 response task. *J Neurosci Off J Soc Neurosci* 13:900–913.
- 18 1070 Schultz W, Apicella P, Scarnati E, Ljungberg T (1992): Neuronal activity in monkey ventral  
19 1071 striatum related to the expectation of reward. *J Neurosci Off J Soc Neurosci*  
20 1072 12:4595–4610.
- 21 1073 Schultz W (1998): Predictive Reward Signal of Dopamine Neurons. *J Neurophysiol* 80:1–27.
- 22 1074 Schultz W (2016a): Dopamine reward prediction-error signalling: a two-component  
23 1075 response. *Nat Rev Neurosci* 17:183–195.
- 24 1076 Schultz W (2016b): Dopamine reward prediction error coding. *Dialogues Clin Neurosci*  
25 1077 18:23–32.
- 26 1078 Schultz W, Dayan P, Montague PR (1997): A Neural Substrate of Prediction and Reward.  
27 1079 *Science* 275:1593–1599.
- 28 1080 Schwartenbeck P, FitzGerald THB, Dolan R (2016): Neural signals encoding shifts in beliefs.  
29 1081 *NeuroImage* 125:578–586.
- 30 1082 Scimeca JM, Katzman PL, Badre D (2016): Striatal prediction errors support dynamic control  
31 1083 of declarative memory decisions. *Nat Commun* 7:ncomms13061.
- 32 1084 Serences JT (2008): Value-based modulations in human visual cortex. *Neuron* 60:1169–  
33 1085 1181.
- 34 1086 Sescousse G, Caldú X, Segura B, Dreher J-C (2013): Processing of primary and secondary  
35 1087 rewards: A quantitative meta-analysis and review of human functional neuroimaging  
36 1088 studies. *Neurosci Biobehav Rev* 37:681–696.
- 37 1089 Seymour B, Daw N, Dayan P, Singer T, Dolan R (2007): Differential Encoding of Losses and  
38 1090 Gains in the Human Striatum. *J Neurosci Off J Soc Neurosci* 27:4826–4831.
- 39 1091 Silvetti M, Verguts T (2012): Reinforcement Learning, High-Level Cognition, and the Human  
40 1092 Brain. [http://www.intechopen.com/books/neuroimaging-cognitive-and-clinical-  
41 1093 neuroscience/reinforcement-learning-high-level-cognition-and-the-human-brain.](http://www.intechopen.com/books/neuroimaging-cognitive-and-clinical-neuroscience/reinforcement-learning-high-level-cognition-and-the-human-brain)
- 42 1094 So N, Stuphorn V (2012): Supplementary Eye Field Encodes Reward Prediction Error. *J*  
43 1095 *Neurosci* 32:2950–2963.
- 44 1096 Späti J, Chumbley J, Brakowski J, Dörig N, Grosse Holtforth M, Seifritz E, Spinelli S (2014):  
45 1097 Functional lateralization of the anterior insula during feedback processing. *Hum*  
46 1098 *Brain Mapp* 35:4428–4439.
- 47 1099 Spicer J, Galvan A, Hare TA, Voss H, Glover G, Casey B (2007): Sensitivity of the Nucleus  
48 1100 Accumbens to Violations in Expectation of Reward. *NeuroImage* 34:455–461.

- 1  
2  
3 1101 Spoomaker VI, Andrade KC, Schröter MS, Sturm A, Goya-Maldonado R, Sämann PG, Czisch  
4 1102 M (2011): The neural correlates of negative prediction error signaling in human fear  
5 1103 conditioning. *NeuroImage* 54:2250–2256.
- 6 1104 Sutton R (1998): Reinforcement Learning: An Introduction. Cambridge, Mass: MIT Press.
- 7 1105 Takemura H, Samejima K, Vogels R, Sakagami M, Okuda J (2011): Stimulus-Dependent  
8 1106 Adjustment of Reward Prediction Error in the Midbrain. *PLOS ONE* 6:e28337.
- 9 1107 Tanaka SC, Doya K, Okada G, Ueda K, Okamoto Y, Yamawaki S (2004): Prediction of  
10 1108 immediate and future rewards differentially recruits cortico-basal ganglia loops. *Nat*  
11 1109 *Neurosci* 7:nn1279.
- 12 1110 Tanaka SC, Samejima K, Okada G, Ueda K, Okamoto Y, Yamawaki S, Doya K (2006): Brain  
13 1111 mechanism of reward prediction under predictable and unpredictable environmental  
14 1112 dynamics. *Neural Netw Off J Int Neural Netw Soc* 19:1233–1241.
- 15 1113 Tobia MJ, Gläscher J, Sommer T (2016): Context-specific behavioral surprise is differentially  
16 1114 correlated with activity in anterior and posterior brain systems. *Neuroreport* 27:677–  
17 1115 682.
- 18 1116 Turkeltaub PE, Eden GF, Jones KM, Zeffiro TA (2002): Meta-analysis of the functional  
19 1117 neuroanatomy of single-word reading: method and validation. *NeuroImage* 16:765–  
20 1118 780.
- 21 1119 Ullsperger M, Cramon DY von (2003): Error Monitoring Using External Feedback: Specific  
22 1120 Roles of the Habenular Complex, the Reward System, and the Cingulate Motor Area  
23 1121 Revealed by Functional Magnetic Resonance Imaging. *J Neurosci* 23:4308–4314.
- 24 1122 Valentin VV, O’Doherty JP (2009): Overlapping prediction errors in dorsal striatum during  
25 1123 instrumental learning with juice and money reward in the human brain. *J*  
26 1124 *Neurophysiol* 102:3384–3391.
- 27 1125 Watanabe N, Sakagami M, Haruno M (2013): Reward Prediction Error Signal Enhanced by  
28 1126 Striatum–Amygdala Interaction Explains the Acceleration of Probabilistic Reward  
29 1127 Learning by Emotion. *J Neurosci* 33:4487–4493.
- 30 1128 Wittmann MK, Kolling N, Akaishi R, Chau BKH, Brown JW, Nelissen N, Rushworth MFS  
31 1129 (2016): Predictive decision making driven by multiple time-linked reward  
32 1130 representations in the anterior cingulate cortex. *Nat Commun* 7:12327.
- 33 1131 Wunderlich K, Rangel A, O’Doherty JP (2009): Neural computations underlying action-based  
34 1132 decision making in the human brain. *Proc Natl Acad Sci* 106:17199–17204.
- 35 1133 Wunderlich K, Symmonds M, Bossaerts P, Dolan RJ (2011): Hedging your bets by learning  
36 1134 reward correlations in the human brain. *Neuron* 71:1141–1152.
- 37 1135 Yacubian J, Gläscher J, Schroeder K, Sommer T, Braus DF, Büchel C (2006): Dissociable  
38 1136 systems for gain- and loss-related value predictions and errors of prediction in the  
39 1137 human brain. *J Neurosci Off J Soc Neurosci* 26:9530–9537.
- 40 1138 Yeung N, Sanfey AG (2004): Independent Coding of Reward Magnitude and Valence in the  
41 1139 Human Brain. *J Neurosci* 24:6258–6264.
- 42 1140 Yu AJ, Dayan P (2005): Uncertainty, Neuromodulation, and Attention. *Neuron* 46:681–692.
- 43 1141 Zalla T, Koehlin E, Pietrini P, Basso G, Aquino P, Sirigu A, Grafman J (2000): Differential  
44 1142 amygdala responses to winning and losing: a functional magnetic resonance imaging  
45 1143 study in humans. *Eur J Neurosci* 12:1764–1770.
- 46 1144 Zhang S, Mano H, Ganesh G, Robbins T, Seymour B (2016): Dissociable Learning Processes  
47 1145 Underlie Human Pain Conditioning. *Curr Biol* 26:52–58.
- 48 1146 Zink CF, Pagnoni G, Martin-Skurski ME, Chappelow JC, Berns GS (2004): Human striatal  
49 1147 responses to monetary reward depend on saliency. *Neuron* 42:509–517.

1148

1149

1150

**Table 1.** Categorisation of fMRI studies into the three RPE components (valence, surprise, signed RPE) and broken down by the relevant fMRI contrast/regressor.

Statistical comparisons	Number	Total	Reference
<b>Valence</b> <b>Pattern A i (NEG&gt;POS)</b>		32	[de Bruijn et al., 2009; Daniel et al., 2011; Demos et al., 2012; van Duijvenvoorde et al., 2014; Elward et al., 2015; Ferdinand and Opitz, 2014; Fouragnan et al., 2015; Gläscher et al., 2009; Haruno et al., 2004; Häusler et al., 2016; Jocham et al., 2016; Kahnt et al., 2010; Katahira et al., 2015; Klein-Flügge et al., 2011; Klein-Flügge et al., 2011; Knutson et al., 2000; Knutson et al., 2001; Koch et al., 2008; Leknes et al., 2011; Losecaat Vermeer et al., 2014; Marsh et al., 2010; Mattfeld et al., 2011; Noonan et al., 2011; O'Doherty et al., 2001; O'Doherty et al., 2003; Rodriguez, 2009; Rolls et al., 2008; Scholl et al., 2015; Seymour et al., 2007; Spicer et al., 2007; Spoomaker et al., 2011; Ullsperger and Cramon, 2003; Yacubian et al., 2006]
Negative > Positive	19		
Negative > No outcomes	9		
Negative correlation with a regressor defining valence RPE (with a binary modulation whereby positive RPE = 1, and negative RPE = -1)	4		
<b>Valence</b> <b>Pattern A ii (POS&gt;NEG)</b>		33	[Amiez et al., 2012; Aron et al., 2004; Bickel et al., 2009; de Bruijn et al., 2009; Canessa et al., 2013; Daniel et al., 2011; van Duijvenvoorde et al., 2014; Elliott et al., 2000; Ernst et al., 2004; Forster and Brown, 2011; Fouragnan et al., 2015; Fujiwara et al., 2009; Häusler et al., 2016; Hester et al., 2008; Hester et al., 2010; Jocham et al., 2016; Katahira et al., 2015; Knutson et al., 2000; Knutson et al., 2001; Knutson et al., 2001; Kumiawan et al., 2013; Losecaat Vermeer et al., 2014; Luking et al., 2014; Paschke et al., 2015; Sarinopoulos et al., 2010; Scholl et al., 2015; Schonberg et al., 2010; Seymour et al., 2007; Späti et al., 2014; Spoomaker et al., 2011; Ullsperger and Cramon, 2003]
Positive > Negative	18		
Positive > No outcomes	9		
Positive correlation with a regressor defining valence RPE (with a binary modulation whereby positive RPE = 1, and negative RPE = -1)	6		
<b>Surprise</b> <b>Pattern B</b>		41	[Allen et al., 2016; Amado et al., 2016; Amiez et al., 2012; Boll et al., 2013; Browning et al., 2010; Chumbley et al., 2014; Daw et al., 2011; Dreher, 2013; Ferdinand and Opitz, 2014; Forster and Brown, 2011; Fouragnan et al., 2015; Fouragnan et al., 2017; Fujiwara et al., 2009; Ide et al., 2013; Iglesias et al., 2013; Jensen et al., 2007; Knutson et al., 2001; Kotz et al., 2015; Leong et al., 2017; Losecaat Vermeer et al., 2014; Manza et al., 2016; McClure et al., 2003; Metereau and Dreher, 2013; Metereau and Dreher, 2015; Meyniel and Dehaene, 2017; Nieuwenhuis et al., 2005; O'Reilly et al., 2013; den Ouden et al., 2012; Poudel et al., 2013; Rodriguez, 2009; Rohe et al., 2012; Rohe and Noppeney, 2015; Rohe and Noppeney, 2015; Rolls et al., 2008; Schwartenbeck et al., 2016; Silvetti and Verguts, 2012; Tobia et al., 2016; Watanabe et al., 2013; Wunderlich et al., 2009; Wunderlich et al., 2011; Yacubian et al., 2006; Zalla et al., 2000; Zhang et al., 2016]
Unsigned RPE ("RL surprise")	12		
Unsigned Bayesian RPE ("Volatility", "Bayesian surprise")	13		
Positive and Negative outcomes > No or low outcomes	9		
"Associability" term of the Pearce et Hall model	2		
Parametric changes in magnitude of surprising positive RPE (unsigned)	3		
Parametric changes in magnitude of surprising negative RPE (unsigned)	2		
<b>Signed RPE</b> <b>Pattern C</b>		38	[Abler et al., 2006; Behrens et al., 2007; van den Bos et al., 2012; Cohen and Ranganath, 2007; Daw et al., 2011; Delgado et al., 2000; Delgado, 2007; Diederer et al., 2017; Diuk et al., 2013; Dunne et al., 2016; Gläscher et al., 2010; Guo et al., 2016; Hare et al., 2008; Ide et al., 2013; Katahira et al., 2015; Leong et al., 2017; Li and Zhang, 2006; Lin et al., 2012; Mattfeld et al., 2011; McClure et al., 2003; Metereau and Dreher, 2013; Metereau and Dreher, 2015; O'Doherty et al., 2003; Pessiglione et al., 2006; Pessiglione et al., 2008; Ribas-Fernandes et al., 2011; Rolls et al., 2008; Schlagenhauf et al., 2013; Schonberg et al., 2010; Scimeca et al., 2016; Seymour et al., 2007; Takemura et al., 2011; Tanaka et al., 2004; Tanaka et al., 2006; Valentin and O'Doherty, 2009; Watanabe et al., 2013; Wunderlich et al., 2011]
Signed RPE (from model-free RL models)	16		
Signed RPE (from model-based RL models)	8		
Signed Bayesian RPE	10		
High positive RPEs > low positive RPEs > low negative RPEs > high negative RPEs	4		

1151

1152

1153 **Table 2.** ALE cluster results for the valence analysis: Pattern A (i) and (ii) (FDR-ID  $P < 0.05$ ,  
 1154 with a minimum volume cluster size of  $50 \text{ mm}^3$ .

Region	R/L	x	y	z	Cluster size	ALE score
<b>Pattern A (i) NEG &gt; POS</b>						
Dorsomedial cingulate cortex (dmCC)	R	2	24	36	12712	0.051
Anterior Insula (aINS)	R	32	24	-2	6120	0.062
-	L	-32	22	-4	4880	0.056
Pallidum	R	12	8	4	3360	0.04
-	L	-14	6	2	2520	0.029
Middle Frontal Gyrus	R	38	4	32	3152	0.029
-	R	30	10	56	488	0.021
-	L	-28	12	60	104	0.019
Inferior Parietal Lobule (IPL)	R	40	-48	42	2416	0.039
-	L	-38	-48	42	2216	0.043
Middle Temporal Gyrus (MTG)	R	60	-28	-6	1192	0.031
Amygdala	R	18	-6	-12	704	0.024
Thalamus	L	-12	-12	10	624	0.025
-	L	-6	-26	8	280	0.023
Habenula	R	2	-20	-18	312	0.022
Dorsolateral Prefrontal Cortex (dlPFC)	L	-44	28	32	360	0.020
-	R	40	34	30	344	0.020
Fusiform Area	L	-40	-62	-10	272	0.023
Precentral Cortex	L	-52	0	34	256	0.021
Dorsomedial Orbitofrontal Cortex (dmOFC)	R	38	58	-2	192	0.020
Dorsomedial Prefrontal Cortex (dmPFC)	R	20	50	4	120	0.018
Superior Temporal Sulcus	R	58	-42	22	120	0.017
<b>Pattern A (ii) (POS &gt; NEG)</b>						
Ventral striatum (vSTR)	L	-12	8	-4	4880	0.052
-	R	8	8	-2	2880	0.038
Ventromedial Prefrontal Cortex (vmPFC)	L	-2	42	0	3416	0.037
Posterior Cingulate Cortex (PCC)	L	0	-32	36	240	0.016
-	L	0	-36	26	88	0.014
Ventrolateral OFC (vlOFC)	R	32	44	-10	144	0.015
Dorsomedial Prefrontal Cortex (dmPFC)	L	-6	-56	14	96	0.016
Medial Prefrontal Cortex (mPFC)	L	-2	46	20	88	0.014

1155

1156



1157 **Table 3.** ALE clusters results for the surprise analysis (FDR-ID  $P < 0.05$ , with a minimum  
 1158 volume cluster size of  $50 \text{ mm}^3$ ).

Region	R/L	x	y	z	Cluster size	ALE score
Anterior mid-cingulate Cortex (aMCC)	R	4	24	34	4072	0.029
Anterior Insula (aINS)	R	32	24	-4	2496	0.050
-	L	-32	20	-4	1544	0.038
Inferior Parietal Lobule (IPL)	R	40	-46	42	1672	0.033
-	L	-40	-48	42	568	0.025
Dorsal Striatum (dSTR)	R	12	8	4	1400	0.034
-	L	-14	10	2	1216	0.021
Middle Temporal Gyrus (MTG)	R	60	-28	-8	648	0.022
Lateral Inferior Frontal Cortex	R	52	10	18	488	0.025
Lateral Central Frontal Gyrus	L	-44	26	30	392	0.019
Precentral Gyrus	R	48	12	34	360	0.019
-	L	-52	0	34	224	0.020
Midbrain	R	2	-20	-18	304	0.021
Dorsal mid-cingulate cortex (dMCC)	R	12	14	42	224	0.019
Hippocampus	R	20	-6	-10	160	0.018
Fusiform Gyrus	L	-40	-60	-10	112	0.017
Mid Occipital Pole	L	-16	-90	-6	112	0.016
Superior Temporal Sulcus	R	60	-40	20	64	0.015

1159

1160

1161 **Table 4.** ALE cluster results for the conjunction analysis of valence and surprise (FDR-ID  $p <$   
 1162 0.05, with a minimum volume cluster size of 50 mm<sup>3</sup>).

Region	R/L	x	y	z	Cluster size	ALE score
Striatum (STR)	R	12	6	4	1082	0.031
-	L	-12	12	4	376	0.021
Anterior Insula (aINS)	L	-32	20	-6	453	0.018
Anterior Mid-cingulate cortex (aMCC)	R	3	22	37	221	0.014
Inferior Parietal Lobule	L	40	-46	42	327	0.014

1163

1164 **Table 5.** ALE cluster results for the contrast analyses of valence and surprise (FDR-pN  $p <$   
 1165 0.05, with a minimum volume cluster size of 50 mm<sup>3</sup>).

Region	R/L	x	y	z	Cluster size	ALE score
<b>Valence vs. Surprise</b>						
Ventral Striatum (vSTR)	L	-10	8	-10	1096	3.29
ventromedial prefrontal cortex (vmPFC)	L	-2	44	0	256	3.29
<b>Positive vs. Surprise</b>						
Ventral Striatum (vSTR)	L	-12	-8	-8	1872	3.29
ventromedial prefrontal cortex (vmPFC)	R	0	46	0	512	3.29
Ventral Striatum (vSTR)	R	8	8	-6	168	3.29
<b>Negative vs. Surprise</b>						
Middle Insula (mINS)	R	40	10	2	544	3.29
Mid Cingulate Cortex (MCC)	R	6	20	42	144	3.29
<b>Surprise vs. Valence</b>						
Anterior Insula (aINS)	R	32	24	-4	1224	3.29
Anterior Insula (aINS)	L	-32	20	-2	112	3.29
Ventral Tegmental Area (VTA)	L	-6	-16	-10	96	3.29
Ventral Tegmental Area (VTA)	R	2	-20	-16	72	3.29
Occipital Lobe	R	24	-80	-6	72	3.29
<b>Surprise vs. Positive</b>						
Anterior Insula (aINS)	R	32	22	-2	1648	3.29
Middle Temporal Gyrus (MTG)	R	40	-46	42	1184	3.29
Anterior Insula (aINS)	L	-32	22	-2	1016	3.29
Inferior Frontal Gyrus	R	52	10	18	184	3.29
Supplementary Motor Area (SMA)	L	-2	12	52	160	3.29
<b>Surprise vs. Negative</b>						
Angular Gyrus	R	40	-46	40	248	3.29
Anterior Insula (aINS)	R	32	28	-6	80	3.29
Dorsal Striatum (dSTR)	R	12	10	2	56	3.29

1166

1167 **Table 6.** ALE clusters results for the signed RPE studies (FDR-ID  $p < 0.05$ , with a minimum  
1168 volume cluster size of  $50 \text{ mm}^3$ ).

Region	R/L	x	y	z	Cluster size	ALE score
Striatum (STR) (encompasses left and right hemispheres)	R	12	10	-4	10888	0.053
Putamen	R	30	-6	8	688	0.024
Anterior Mid-cingulate Cortex (aMCC)	R	6	26	46	160	0.018
-	L	-2	14	40	120	0.016
Anterior Cingulate Cortex (ACC)	R	4	36	20	112	0.017
Ventromedial prefrontal (vmPFC)	L	0	34	0	64	0.015
Lateral Inferior Frontal Gyrus (IIFC)	L	-46	4	24	64	0.016

1169

1170 **Table 7.** ALE cluster results for the contrast analyses of signed RPE and valence as well as  
1171 signed RPE and surprise (FDR-pN  $p < 0.05$ , with a minimum volume cluster size of  $50 \text{ mm}^3$ ).

Region	R/L	x	y	z	Cluster size	ALE score
<b>Positive – Signed RPE</b>						
Ventromedial Prefrontal Cortex (vmPFC)	R	2	44	-15	160	3.29
<b>Signed RPE - Positive</b>						
No significant						
<b>Negative – Signed RPE</b>						
Middle Insula (mINS)	R	40	12	0	528	3.29
Dorsal Middle Cingulate Cortex (dMCC)	R	6	22	36	208	3.29
Middle Insula (mINS)	L	-38	18	-4	184	3.29
Habenula	L	-2	-26	8	168	2.58
Thalamus	R	8	-10	5	96	2.58
<b>Signed RPE - Negative</b>						
Ventral Striatum (vSTR)	R	10	10	-6	2208	3.29
<b>Valence – Signed RPE</b>						
Ventromedial Prefrontal Cortex (vmPFC)	R	2	44	-12	760	3.29
Middle Insula (mINS)	R	40	12	2	568	2.58
Dorsal Middle Cingulate Cortex (dMCC)	R	6	24	38	480	2.58
<b>Signed RPE - Valence</b>						
Ventral Striatum (vSTR)	R	12	16	-2	184	3.29
<b>Surprise – Signed RPE</b>						
Anterior Insula (aINS)	L	-34	22	0	704	3.29
Anterior Midcingulate Cortex (aMCC)	R	0	14	52	136	3.29
Pre supplementary motor area (preSMA)	R	0	14	52	136	3.29
Anterior Insula (aINS)	R	38	18	-2	88	3.29

1172

---

<b>Signed RPE - Surprise</b>						
Ventral Striatum (vSTR)	L	-10	8	-10	904	3.29
Ventral Striatum (vSTR)	R	12	14	-3	192	3.29
Ventral Striatum (vSTR)	R	4	6	-6	72	3.29

---

For Peer Review

1  
2  
3 1173 **Figure Legends**

4  
5 1174

6  
7 1175 **Figure 1.** Hypothesized profiles for BOLD responses as function of the three RPE  
8  
9 1176 components. Pattern A (i and ii) describe the two categorical valence responses (orange and  
10  
11 1177 blue colours indicate (i) responses being greater for negative compared to positive outcomes  
12  
13 1178 [NEG > POS] and (ii) responses being greater for positive compared to negative outcomes  
14  
15 1179 [POS > NEG]). Pattern B captures surprise effects with greater responses to higher outcome  
16  
17 1180 deviations from expectations, independent of the sign (valence) of the RPE. Pattern C shows  
18  
19 1181 a monotonically increasing response profile consistent with a signed RPE representation.

20  
21 1182

22  
23 1183 **Figure 2.** Results of whole-brain ALE analysis along the valence component. Overlays of  
24  
25 1184 brain areas activated by correlations with NEG > POS (blue) and POS > NEG (orange)  
26  
27 1185 (Pattern A (i) and (ii), respectively; Fig. 1) (P-values corrected with FDR-ID [FID] and FDR-  
28  
29 1186 pN [FRN] < 0.05 and a minimum cluster volume of 50 mm<sup>3</sup>). Representative slices are  
30  
31 1187 shown with MNI coordinates given below each image.

32  
33 1188

34  
35 1189 **Figure 3.** Results of the whole brain ALE analysis for the surprise component of RPE  
36  
37 1190 (pattern B, Figure 1). Overlay of brain areas activated by all analyses representing direct or  
38  
39 1191 indirect measures of the surprise component of RPE (P-values corrected with FDR-ID [FID]  
40  
41 1192 and FDR-pN [FRN] < 0.05 and a minimum cluster volume of 50 mm<sup>3</sup>). Representative slices  
42  
43 1193 are shown with MNI coordinates given below each image.

44  
45 1194

46  
47 1195 **Figure 4.** Results of the ALE conjunction analysis between valence and surprise (purple).  
48  
49 1196 The regions identified earlier with separate ALE analyses along the valence (NEG > POS:  
50  
51 1197 blue, POS > NEG: orange) and surprise (green) components are shown for comparison  
52  
53 1198 purposes. P-values were corrected with FDR-pN [FRN] < 0.05 and a minimum cluster  
54  
55 1199 volume of 50 mm<sup>3</sup> for the initial maps. Representative slices are shown with MNI coordinates  
56  
57 1200 given bellow each image.

1  
2  
3 1201 **Figure 5.** Results of the ALE contrast analyses for [valence – surprise] (left panel) and  
4 1202 [surprise – valence]. P-values were corrected with FDR-pN [FRN] < 0.05 and a minimum  
5 1203 cluster volume of 50 mm<sup>3</sup> for the initial maps. Representative slices are shown with MNI  
6 1204 coordinates given bellow each image.  
7  
8  
9

10  
11 1205

12  
13 1206 **Figure 6.** Results of whole brain ALE analysis for signed RPE. Overlay of brain areas  
14 1207 activated by positive correlation with signed RPE (P-values corrected with FDR-ID [FID] and  
15 1208 FDR-pN [FRN] < 0.05 and a minimum cluster volume of 50 mm<sup>3</sup>). Representative slices are  
16 1209 shown with MNI coordinates given bellow each image.  
17  
18  
19

20  
21 1210

22  
23 1211 **Figure 7.** Results of the ALE conjunction analysis for all components of RPE. Overlay of  
24 1212 brain areas individually activated by (1) valence (orange), (2) surprise (green), and (3)  
25 1213 signed RPE (red), with P-values corrected with FDR-pN [FRN] < 0.05 and a minimum cluster  
26 1214 volume of 50 mm<sup>3</sup> for the initial maps. Importantly, the overlap between the three analyses,  
27 1215 shown in white, also corresponds to the only cluster found for the ALE conjunction analysis  
28 1216 between valence/surprise vs. signed RPE. MNI coordinates are given below each image.  
29  
30  
31  
32  
33

34  
35 1217

36 1218 **Figure 8.** Results of the ALE contrast analyses for [signed RPE – positive valence] (left  
37 1219 panel), [signed RPE – negative valence] (middle panel) and [signed RPE – (positive +  
38 1220 negative valence)] (right panel). P-values were corrected with FDR-pN [FRN] < 0.05 and a  
39 1221 minimum cluster volume of 50 mm<sup>3</sup> for the initial maps. Representative slices are shown with  
40 1222 MNI coordinates given bellow each image.  
41  
42  
43  
44  
45

46  
47 1223  
48  
49  
50  
51  
52  
53  
54  
55  
56  
57  
58  
59  
60

1  
2  
3  
4  
5  
6  
7  
8  
9  
10  
11  
12  
13  
14  
15  
16  
17  
18  
19  
20  
21  
22  
23  
24  
25  
26  
27  
28  
29  
30  
31  
32  
33  
34  
35  
36  
37  
38  
39  
40  
41  
42  
43  
44  
45  
46  
47  
48  
49  
50  
51  
52  
53  
54  
55  
56  
57  
58  
59  
60

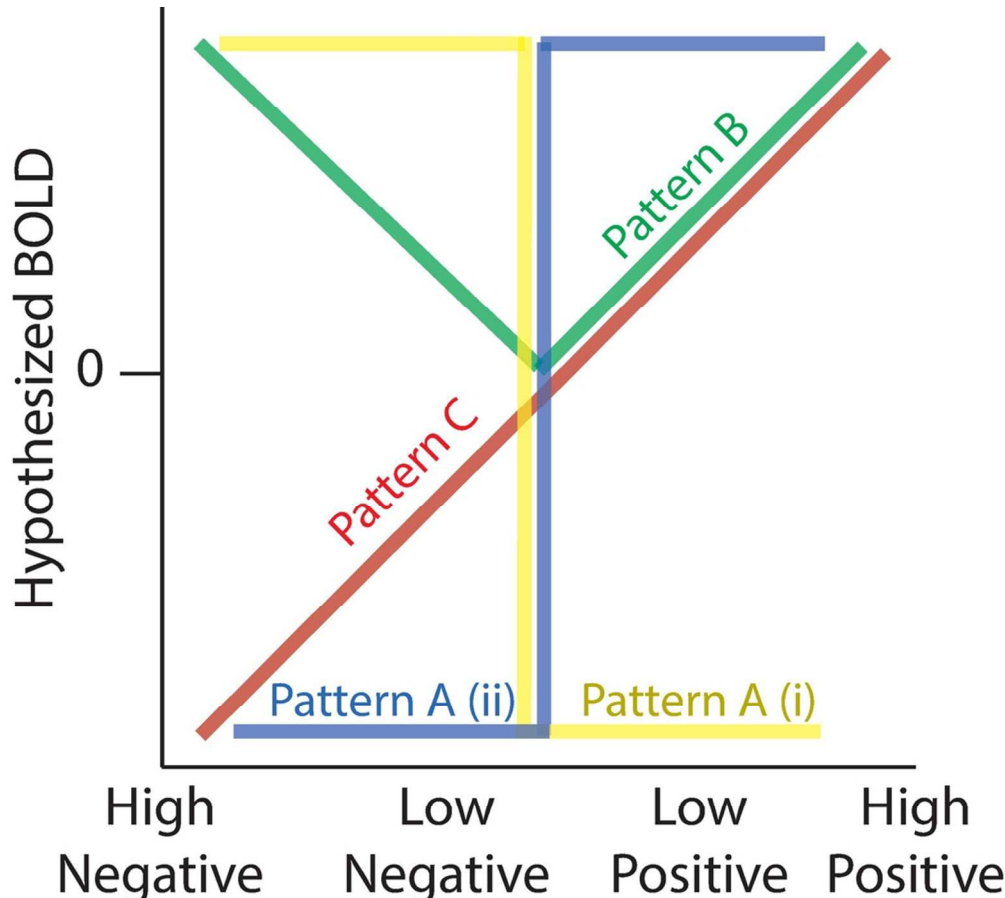


fig.1

91x81mm (300 x 300 DPI)



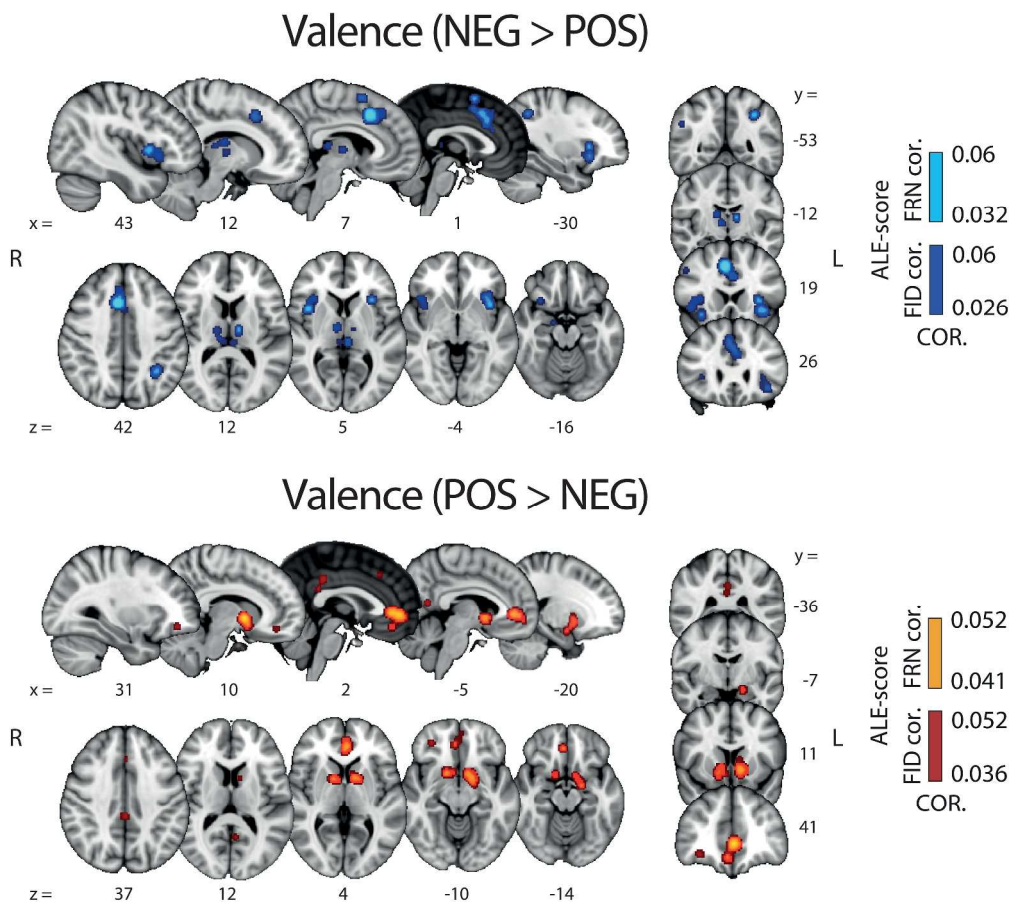


fig.2

378x339mm (300 x 300 DPI)





1  
2  
3  
4  
5  
6  
7  
8  
9  
10  
11  
12  
13  
14  
15  
16  
17  
18  
19  
20  
21  
22  
23  
24  
25  
26  
27  
28  
29  
30  
31  
32  
33  
34  
35  
36  
37  
38  
39  
40  
41  
42  
43  
44  
45  
46  
47  
48  
49  
50  
51  
52  
53  
54  
55  
56  
57  
58  
59  
60

### Surprise

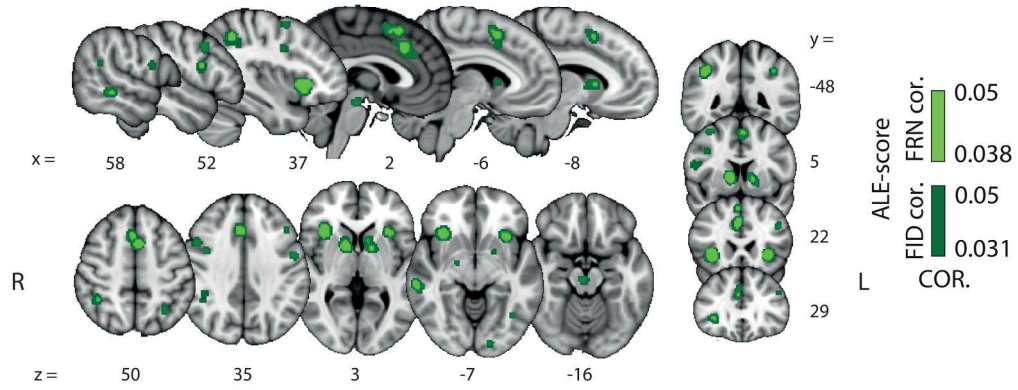


fig.4

203x100mm (300 x 300 DPI)

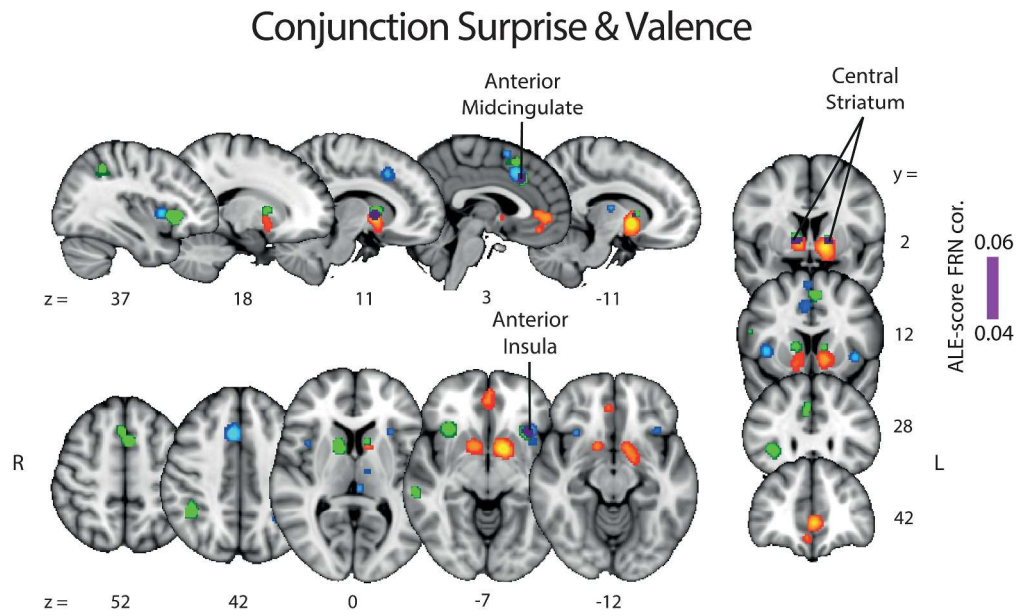


fig.4

285x172mm (300 x 300 DPI)

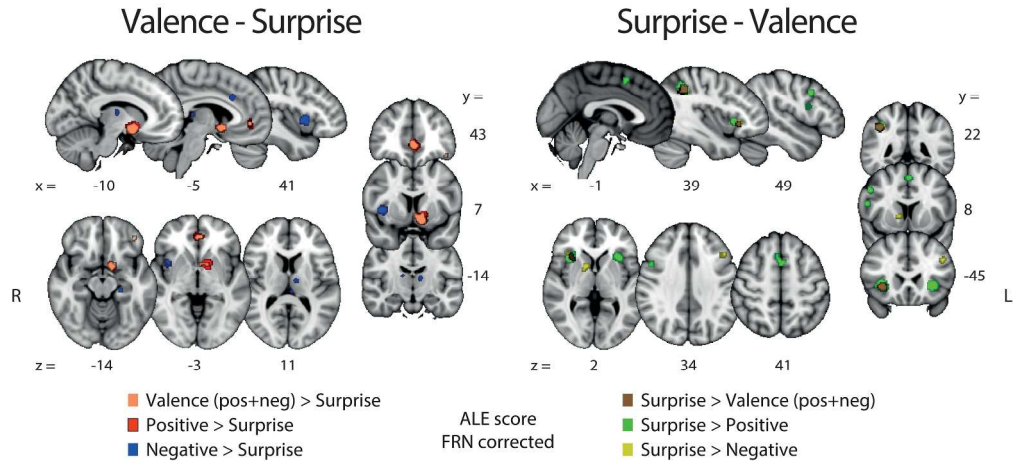


fig.5

252x115mm (300 x 300 DPI)

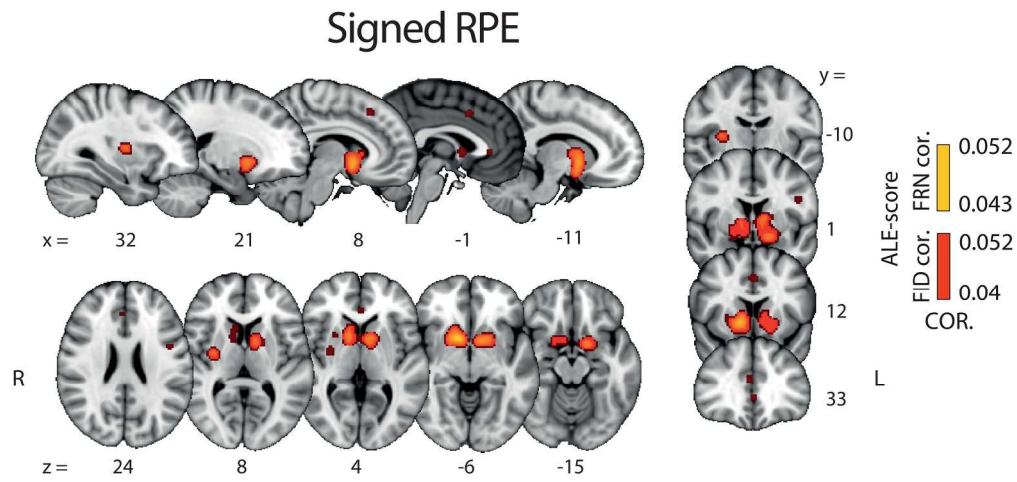


fig.6

207x98mm (300 x 300 DPI)

1  
2  
3  
4  
5  
6  
7  
8  
9  
10  
11  
12  
13  
14  
15  
16  
17  
18  
19  
20  
21  
22  
23  
24  
25  
26  
27  
28  
29  
30  
31  
32  
33  
34  
35  
36  
37  
38  
39  
40  
41  
42  
43  
44  
45  
46  
47  
48  
49  
50  
51  
52  
53  
54  
55  
56  
57  
58  
59  
60

### Conjunction Surprise & Valence & Signed PE

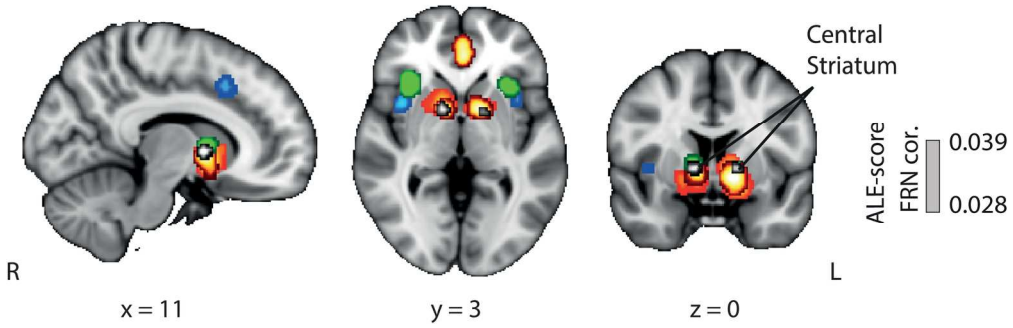


fig.7

164x66mm (300 x 300 DPI)

Peer Review

1  
2  
3  
4  
5  
6  
7  
8  
9  
10  
11  
12  
13  
14  
15  
16  
17  
18  
19  
20  
21  
22  
23  
24  
25  
26  
27  
28  
29  
30  
31  
32  
33  
34  
35  
36  
37  
38  
39  
40  
41  
42  
43  
44  
45  
46  
47  
48  
49  
50  
51  
52  
53  
54  
55  
56  
57  
58  
59  
60

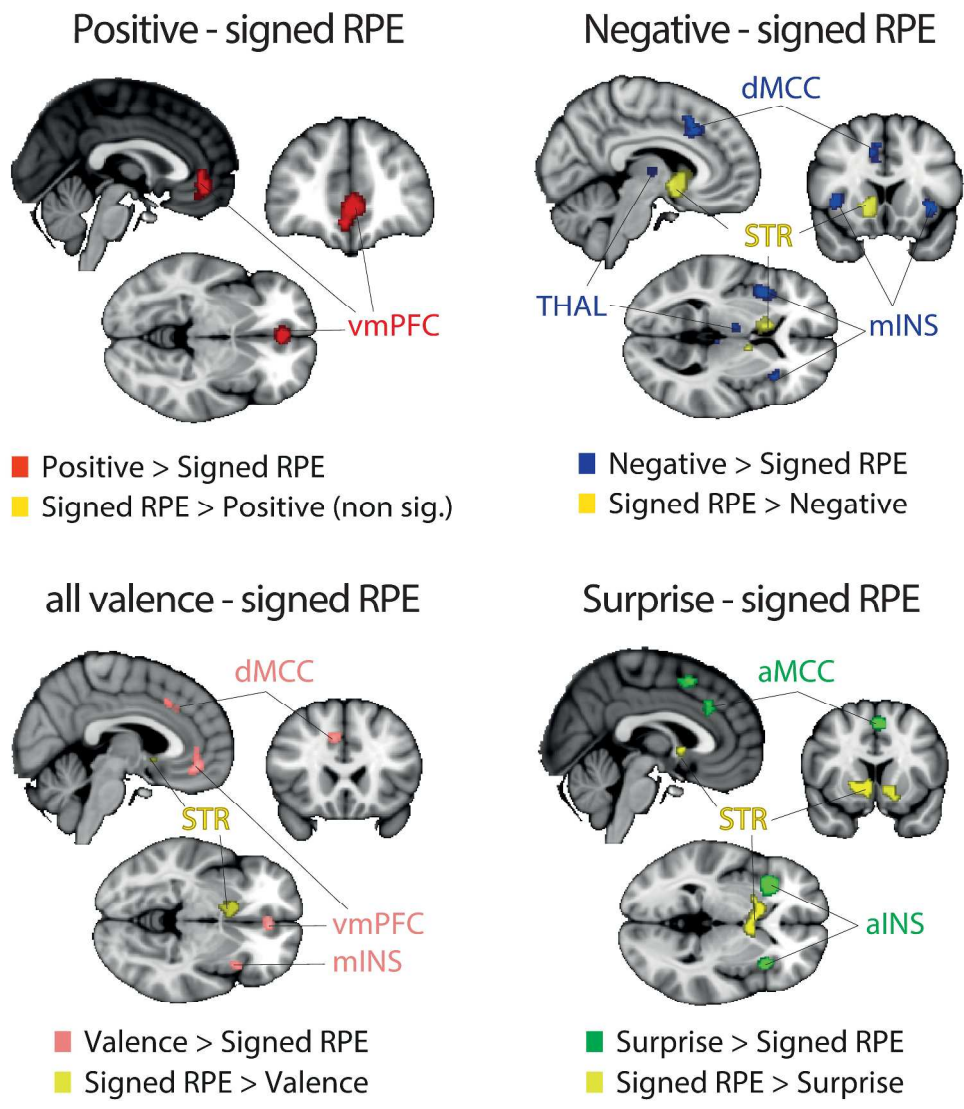


fig.8

366x400mm (300 x 300 DPI)